IL-17 levels have been shown to be significantly higher in the cerebrospinal fluid of patients with active optico-spinal MS (Ishizu et al., 2005) and in the CNS of EAE mice (Hofstetter et al., 2005). The effects of IL-17 on CNS cells, however, are unclear. In order to uncover the contribution of IL-17 to inflammatory demyelination in the CNS, we have examined the effects of IL-17 on microglia, which function as antigen-presenting cells and effector cells in the CNS during inflammatory demyelination.

2. Materials and methods

2.1. Reagents

Lipopolysaccharide (LPS), human recombinant transforming growth factor (TGF)-β, and mouse recombinant IL-17 and IL-23 were obtained from Sigma-Aldrich (St. Louis, MO, USA). Mouse recombinant IL-1β, TNFα, and IFNγ were purchased from Techne (Minneapolis, MN, USA). Sulfonylamide, *N*-(1-naphthyl)ethylenediamine, and phosphate for Griess reagent (Ignarro et al., 1987) were also purchased from Sigma-Aldrich.

2.2. Cell culture

The protocols for the animal experiments were approved by the Animal Experiment Committee of Nagoya University. All primary cultures were prepared from C57BL/6J mice (Japan SLC, Hamamatsu, Shizuoka, Japan). Microglia were isolated from primary mixed glial cell cultures prepared from newborn mice on day 14 using the "shaking off" method as previously described (Suzumura et al., 1987); the purity of the cultures was almost 100%, as determined by immunostaining with anti-CD11b antibodies. The cultures were maintained in Dulbecco's modified Eagle's minimum essential medium (Sigma-Aldrich) supplemented with 10% fetal calf serum (JRH Biosciences, Lenexa, KS, USA), 5 μg/ml bovine insulin (Sigma), and 0.2% glucose.

Astrocyte-enriched cultures were prepared as described previously (Kuno et al., 2006). Briefly, the mixed glial cell cultures were trypsinized after the microglia were collected, and replated in Petri dishes. After this procedure was repeated three times, the cultures that had undergone four passages were used as the astrocyte-enriched cultures. The purity of the cultures were more than 80% as determined by immunostaining with anti-glial fibrillary acidic protein (GFAP). Peritoneal macrophages were collected from mice intraperitoneally injected with thioglycolate 48 h prior to collection. T cell-rich lymphocytes were separated from mouse spleens. Neuronal cultures were prepared from mice at embryonic day 17 as described previously (Takeuchi et al., 2005). Briefly, cortices were dissected and freed of meninges. Cortical fragments were dissociated into single cells using dissociation solution, and they were resuspended in Nerve-Cell Culture Medium (serum-free conditioned medium from 48-h rat astrocyte confluent cultures based on Dulbecco's modified Eagle's minimum essential medium/F-12 with N2 supplement, Sumitomo Bakelite, Akita, Japan). The purity of the cultures was more than 95% as determined by NeuN-specific immunostaining.

2.3. Expression of IL-17 receptors

The mRNA expression of the IL-17 receptor was examined using reverse transcription-polymerase chain reactions (RT-PCRs). Microglia, astrocytes, or neurons were cultured for 3 days before total cellular RNA was extracted using an RNase Mini Kit (Qiagen). cDNA encoding the IL-17 receptor was examined by RT-PCR analysis using SuperScript II (Invitrogen), AmpliTaq DNA polymerase (Applied Biosystems), and the specific primers shown in Table 1. Amplification within the linear range using 5 μl of each cDNA sample was achieved following 30 cycles in a DNA thermal cycler under conditions that were optimized for each set of primers.

The protein level of IL-17 receptor expression was examined using Western blot analysis. Samples (20 μg/well) were electrophoresed on 7.5% SDS-polyacrylamide gels (Invitrogen) according to the Laemmli method (Laemmli and Favre, 1973). After electrophoresis, proteins were transferred from the gels to nitrocellulose membranes (Amersham Bioscience, Buckinghamshire, UK) using standard procedures (Towbin et al., 1979). Nonspecific binding was blocked with 5% nonfat dry milk in TBST buffer (5 mM Tris–HCl, pH 7.6, 136 mM NaCl, 0.05% Tween 20) for 1 h. Blots were incubated for 12 h at 4 °C with rat anti-mouse IL-17 receptor antibody (R&D Systems) (1:1000 dilution). Blots were washed four times in TBST: the first time for 20 min and 10 min each time thereafter. We then incubated the washed blots for 1 h at room temperature with a

Table 1
Primer sequences used for RT-PCR analysis

GAPDH sense, 5′-ACTCACGGGAAATTCAACG
GAPDH antisense, 5′-CCCTGTTGCTGTAGCCGTA
IL-17R sense, 5′-CTAAACTGCACGGTCAAGAAT
IL-17R antisense, 5′-ATGAACCAGTACACCCAC
TNFα sense 5′-ATGAGCACAGAAAGCATGATCCGC
TNFα antisense 5′-CCAAAGTAGACCTGCCCGGACTC
IL-1β sense, 5′-ATGGCAACTGTTCCTGAACTCAACT
IL-1β antisense, 5′-CAGGACAGGTATAGATTCTTTCCTTT
IL-6 sense, 5′-ATGAAGTTCCTCTCTGCAAGAGACT
IL-6 antisense, 5′-CACTAGGTTTGCCGAGTAGGATCTC
MIP-2 sense, 5′-CCGGCTCCTCAGTGCTG
MIP-2 antisense, 5′-GGTCAGTTAGCCTTGCCTTT
IL-17 sense, 5′-CAGGACGCGCAAAACATGA
IL-17 antisense, 5′-GCAACAGCATCAGAGAGACACAGAT
iNOS sense, 5′-CCCTTCCGAAGTTTCTGGCAGCAGC
iNOS antisense, 5′-GGCTGTCAGAGCCTCGTGGCTTTGG
NGF sense, 5′-CATAGCGTAATGTCCATGTTGTTCT
NGF antisense, 5′-CTTCTCATCTGTTGTCAACGC
BDNF sense, 5′-AGCCTCCTCTGCTCTTTCTG
BDNF antisense, 5′-TTGTCTATGCCCCTGCAGCC
GDNF sense, 5′-ATTTTATTCAAGGCCACCATTA
GDNF antisense, 5′-GATACATCCACACCGTTTTAGC
MHC class II antigen sense, 5′-AAGAAGGAGACTGTCTGGATGC
MHC class II antigen antisense, 5′-TGAATGATGAAGATGGTGCCC
ICAM-1 sense, 5′-TTCACACTGAATGCCAGCTC
ICAM-1 antisense, 5′-GTCTGCTGAGACCCCTCTTG
VCAM-1 sense, 5′-ATTTTCTGGGGCAGGAAGTT
VCAM-1 antisense, 5′-ACGTCAGAACAACCGAATCC

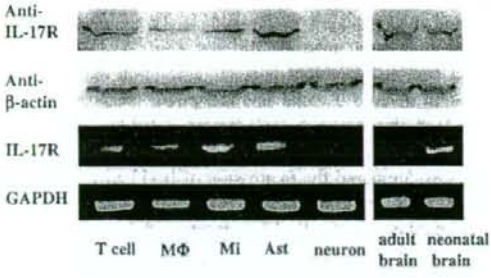

Fig. 1. Expression of IL-17 receptor mRNA and protein in neural cells. Microglia and astrocytes along with splenic T cells and macrophages express IL-17 receptor mRNA and protein, whereas neurons do not. MΦ, macrophages; Mi, microglia; Ast, astrocytes (left panel). The mRNA expression of IL-17 receptor in adult brain was lower than that of neonatal, but protein level of IL-17 receptor was the same as neonatal (right panel).

1:5000 dilution of peroxidase-conjugated, anti-rat IgG secondary antibody (Amersham Bioscience) followed by an additional rinse. IL-17 receptor was detected by ECL (Amersham Bioscience). The molecular weight of IL-17 receptor was determined by running molecular weight markers (Invitrogen) in an adjacent lane. Spleen cells served as a positive control.

2.4. Effects of IL-17 on the production of cytokines, neurotrophic factors and NO by microglia

Microglia and astrocytes were cultured in 24-well plates at a concentration of 1×10^6 cells/ml with or without 1 μg/ml LPS for 24 to 72 h in presence of various doses of IL-17 (1–100 ng/ml). The supernatants were then collected and stored at −80 °C until they were assessed. Total cellular RNA was extracted from remaining cells using an RNase Mini Kit (Qiagen). cDNAs encoding mouse TNFα, IL-1β, IL-6, iNOS, MIP-2 (the functional analogue of human IL-8), Nerve growth factor (NGF), glial cell line-derived neurotrophic factor (GDNF), brain-derived neurotrophic factor (BDNF) and IL-17 were generated and amplified in RT-PCRs as described above using the specific primers shown in Table 1.

Cytokine production was measured using ELISA kits specific for TNFα, IL-6 (Techne), MIP-2, and IL-17 (R&D).

Cellular levels of NGF and BDNF in the microglia were also assessed as follows: stimulated microglial cultures were washed four times in cold PBS, the cells were lysed using sonication in ice-cold PBS containing protease inhibitors (complete mini EDTA-free; Roche, Mannheim, Germany), and the lysates were assayed for cellular NGF and BDNF using ELISA kits specific for NGF and BDNF (Promega, WI, USA). Cytoplasmic GDNF content was measured by an enzyme immunoassay (EIA) as described (Nitta et al., 1999). The EIA system for GDNF was based on the method originally developed for the EIA of NGF, BDNF, and NT-3 (Furukawa et al., 1983; Kaechi et al., 1993; Nitta et al., 1999; Nitta et al., 2004). Antibodies against GDNF were produced by immunizing rabbits with purified human recombinant GDNF. GDNF protein (0.5 mg) in phosphate-buffered saline (PBS; 5 ml) was emulsified with an equal volume of Freund's adjuvant and injected intradermally into rabbits four times at 2-week intervals. Animals were exsanguinated 1 week after the final injection. To affinity purify the antibody, antiserum (1 ml) first was loaded onto a GDNF-linked column (1-ml bed volume; Affi-Gel 10; Bio-Rad, Hercules, CA). After extensive sequential washing with three buffers, 0.1 M Tris–HCl (pH 7.4) containing 0.9% NaCl, 0.05 M borate buffer (pH 8.0), and 0.05 mM sodium acetate buffer (pH 5.0), the bound antibodies were eluted with a 0.1 M glycine–HCl buffer (pH 2.0). A part of the purified anti-GDNF antibody preparation was eluted and biotinylated. The detection limit of the EIAs was as low as 1 pg/ml.

NO production was determined using the Griess reaction as described (Pollock et al., 1991). Briefly, 50-μl aliquots of the supernatants were mixed with an equal volume of Griess reagent (0.1% *N*-ethylenediamine dihydrochloride, 1% sulfanilamide, and 2.5% phosphoric acid) and incubated for 5 min at room temperature. The absorbance at 540 nm was measured

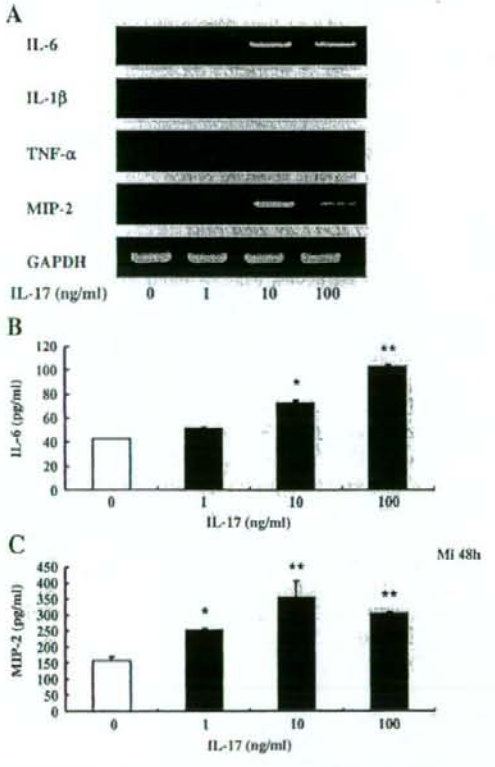

Fig. 2. The effects of IL-17 on cytokine production by microglia. Microglia were treated with IL-17 for 48 h. (A) At concentrations greater than 1 ng/ml, IL-17 induced the expression of IL-6 and MIP-2 mRNA. Similar results were obtained for IL-6 (B) and MIP-2 (C) protein using specific ELISAs. The values shown are the means ± S.D. $^*P<0.05$ and $^{**}P<0.01$ compared with untreated microglia. The data represent typical samples performed in triplicate in three independent experiments.

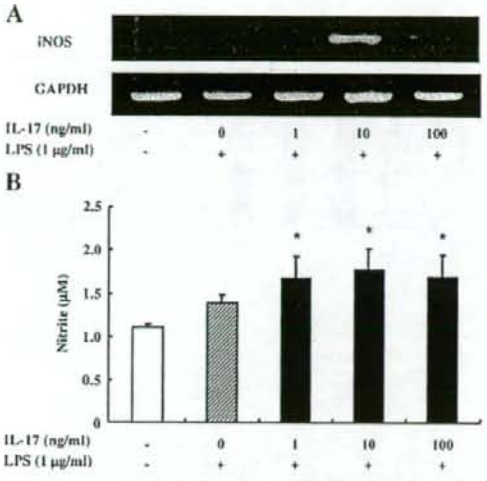

Fig. 3. The effects of IL-17 on NO production and iNOS expression in LPS-stimulated microglia. Microglia were stimulated with LPS for 48 h in the presence of various concentrations of IL-17. IL-17 enhanced iNOS mRNA expression (A) and NO production (B). The values shown are the means±S.D. $^*P<0.05$ compared with LPS-stimulated microglia in the absence of IL-17. The data represent typical samples performed in triplicate in three independent experiments.

using a microtiter plate reader. Nitrite concentrations were calculated from a $NaNO_2$ standard curve.

2.5. Production of IL-17 by glial cells

Microglia and astrocytes were cultured for 72 h in 6-well plates at a concentration of 1×10^6 cells/ml with various doses of IL-23 (1–100 ng/ml). The culture supernatants were then collected and stored at −80°C until they were assessed. IL-17 production was measured using an ELISA kit specific for murine IL-17 (R&D). Total cellular RNA was extracted from the remaining cells using an RNase Mini Kit (Qiagen). cDNAs encoding mouse IL-17 were amplified using RT-PCRs as described above and the specific primers shown in Table 1. In some experiments, cytoplasmic levels of IL-17 in the microglia were also assessed as follows: stimulated microglial cultures were washed four times in cold PBS, the cells were lysed using sonication in ice-cold PBS containing protease inhibitors (complete mini EDTA-free; Roche, Mannheim, Germany), and the lysates were assayed for cellular IL-17 using ELISAs.

3. Results

3.1. Expression of the IL-17 receptor

Increased levels of IL-17 have been observed in the cerebrospinal fluid from patients with active MS as well as in the CNS of EAE mice. Thus, we assessed the expression of IL-17 receptor in CNS cells. RT-PCR demonstrated that neonatal microglia and astrocytes along with splenic T cells and peripheral macrophages expressed IL-17 receptor mRNA, whereas embryonic neurons did not (Fig. 1). Western blot analysis demonstrated that neonatal microglia and astrocytes along with splenic T cells and peripheral macrophages expressed IL-17 receptor protein, whereas embryonic neurons did not (Fig. 1).

We next compared the expression of IL-17 receptor mRNA and protein in adult brain with that of neonatal brain. The expression of mRNA for IL-17 receptor in adult brain was lower than that of neonatal, but protein level of IL-17 receptor was almost identical in these 2 samples (Fig. 1, left panel).

3.2. Effects of IL-17 on microglia

We then assessed the effects of IL-17 on microglia. IL-17 induced the mRNA expression of the inflammatory cytokines IL-6 and MIP-2 with maximum induction observed at 10 ng/ml (Fig. 2A). IL-17, however, did not significantly induce the expression of mRNA encoding IL-1β or TNFα. Upregulation of the expression of IL-6 and MIP-2 protein by IL-17 was confirmed with ELISAs; IL-17 at a concentration of 10 ng/ml or greater significantly increased the production of IL-6 and MIP-2 by microglia (Fig. 2B), whereas IL-1β and TNFα were not detected in the supernatants (data not shown). Although IL-17 by itself did not induce the expression of iNOS mRNA and NO production in unstimulated microglia, it enhanced iNOS mRNA expression and NO production in LPS-stimulated microglia; the maximum increase was observed with 10 ng/ml IL-17 (Fig. 3). In addition, IL-17 dose-dependently upregulated the expression of neurotrophic factors NGF, BDNF, and GDNF (Figs. 4 and 5). IL-17 itself did not induce the expression of mRNA encoding class II major histocompatibility complex (MHC) antigen or cell adhesion molecules (data not shown). On the other hand, the expression of intercellular adhesion molecule (ICAM)-1 and vascular cell adhesion molecule (VCAM)-1 mRNA was upregulated in INFγ-stimulated microglia following treatment with IL-17, whereas it did not affect the expression of class II MHC antigen in these cells (Fig. 6). In contrast to the proinflammatory effects, IL-17 increased the expression of neurotrophic factors in microglia, which may contribute to anti-inflammatory defense mechanisms in the CNS and implies that microglia have multiple functions.

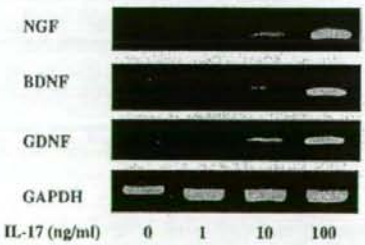

Fig. 4. The effects of IL-17 on the expression of mRNA coding for neurotrophic factors in microglia. Microglia were treated with IL-17 for 72 h. IL-17 dose-dependently induced the expression of NGF, BDNF, and GDNF mRNA.

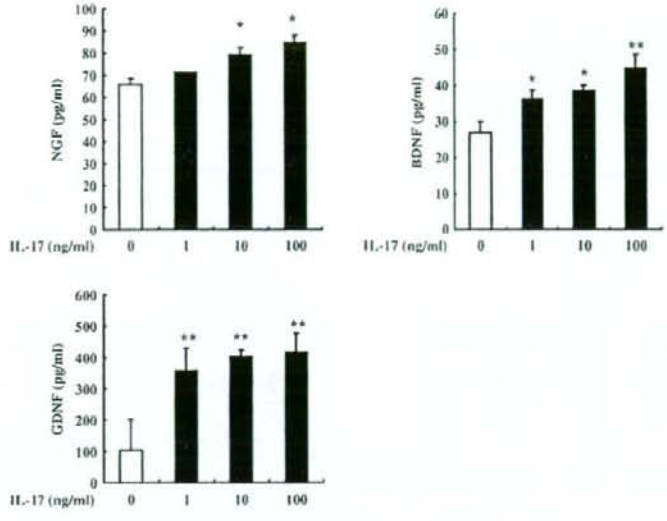

Fig. 5. The effects of IL-17 on the expression of neurotrophic factors in microglia. Microglia were treated with IL-17 for 72 h. IL-17 dose-dependently induced the expression of NGF, BDNF, and GDNF. The values shown are the means ± S.D. *$P < 0.05$ and **$P < 0.01$ compared with untreated microglia. The data represent typical samples performed in triplicate in three independent experiments.

3.3. Production of IL-17 by microglia

IL-17 is reported to be a T cell-specific cytokine (Yao et al., 1995). A study that analyzed human astrocytes using cDNA microarrays, however, suggested that CNS cells produce IL-17 (Meeuwsen et al., 2003). Thus, we assessed IL-17 production in glial cells. Although unstimulated microglia did not express mRNA coding for IL-17, IL-23 induced IL-17 mRNA expression in microglia in a dose-dependent manner. Because ELISAs failed to detect IL-17 in the supernatant of IL-23-stimulated microglia, we measured the cytoplasmic levels of IL-17 in IL-23-stimulated microglia. IL-23 (≥1 ng/ml) significantly increased the cytoplasmic level of IL-17 in a dose-dependent manner (Fig. 7). IL-1β (≥1 ng/ml) also induced the expression of IL-17 mRNA and increased the cytoplasmic level of IL-17 in microglia; maximum induction was observed at 10 ng/ml (Fig. 8). On the contrary, stimulation with IL-23 or IL-23 and IL-1β did not induce IL-17 mRNA expression in astrocytes (data not shown). In the presence of IL-6, TGF-β derived from regulatory T cells induces upregulation of IL-23 receptor expression in Th17 cells (Ivanov et al., 2006). Neither IL-6 nor TGF-β, however, enhanced IL-17

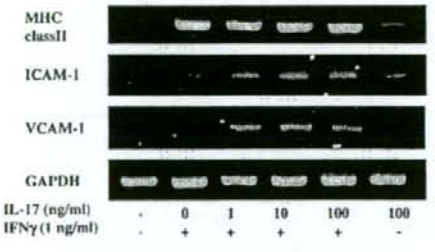

Fig. 6. The effects of IL-17 on the expression of mRNA encoding MHC antigen and adhesion molecules. Microglia were stimulated with IFNγ for 48 h in the presence of various concentrations of IL-17. IL-17 enhanced ICAM-1 and VCAM-1 mRNA expression in INFγ-stimulated microglia, whereas it did not affect MHC class II antigen mRNA levels in these cells.

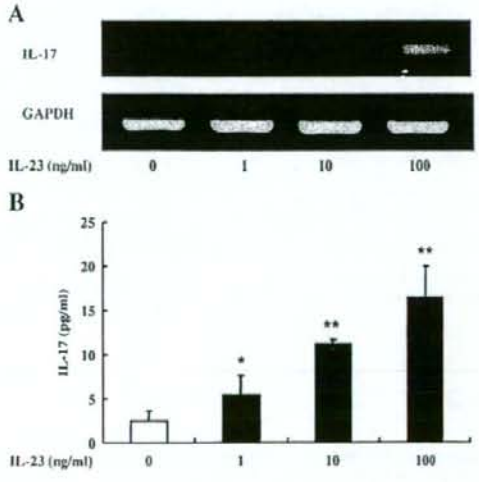

Fig. 7. IL-23 induces IL-17 production by microglia. Microglia were stimulated with various concentrations of IL-23 for 72 h. IL-23 dose-dependently induced IL-17 mRNA expression (A) and increased cytoplasmic IL-17 levels in microglia (B). The values shown are the means ± S.D. *$P < 0.05$ and **$P < 0.01$ compared with untreated microglia. The data represent typical samples performed in triplicate in three independent experiments.

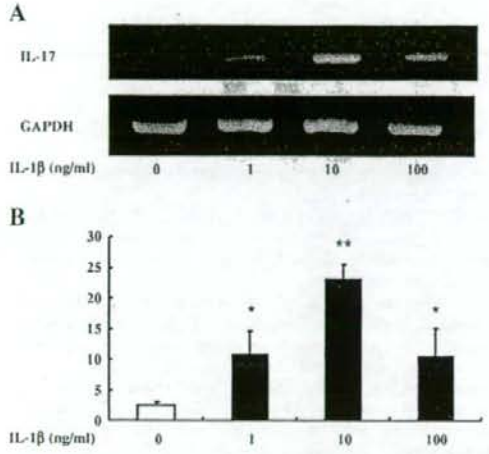

Fig. 8. IL-1β induces IL-17 production by microglia. Microglia were stimulated with various concentrations of IL-1β for 72 h. IL-1β induced IL-17 mRNA expression (A) and increased cytoplasmic IL-17 levels in microglia (B). The values shown are the means±S.D. $^{*}P<0.05$ and $^{**}P<0.01$ compared with untreated microglia. The data represent typical samples performed in triplicate in three independent experiments.

production in unstimulated microglia or in IL-23-stimulated microglia (data not shown). Stimulation with both IL-6 (100 ng/ml) and TGF-β (10 ng/ml) also failed to enhance the level of IL-17 produced by IL-23-stimulated microglia (data not shown).

4. Discussion

IL-17 has been associated with various autoimmune diseases, although its regulation and functional roles remain to be clarified. Antibodies specific for IL-17 reportedly inhibit chemokine expression in the brain during EAE, whereas overexpression of IL-17 in lung epithelia results in chemokine production and leukocyte infiltration. Thus, IL-17 expression characterizes a unique T helper lineage that regulates tissue inflammation (Park et al., 2005). Here we have evaluated the effects of IL-17 on neural cells *in vitro*. In the CNS, microglia and astrocytes express IL-17 receptors, whereas neurons do not. We then examined the effects of IL-17 on microglia—the antigen-presenting effector cells that can induce autoimmune inflammatory processes in the CNS. Because both IL-4 and IFNγ negatively regulate the production of IL-17 by T helper cells during the effector phase, Th17 cells may have roles that are distinct from those of Th1 and Th2 cells. The effects of IL-17 on microglia, however, are similar to those of Th1 cytokines; IL-17 enhanced inflammatory cytokine and chemokine production by microglia. IL-17 did not affect IFNγ-induced MHC class II antigen expression by microglia, whereas it increased the IFNγ-induced expression of adhesion molecules by these cells. IL-17 by itself did not induce iNOS expression or NO production, although it enhanced both of these phenomena in LPS-stimulated microglia. In rodent astrocytes, it has been shown that IL-17 enhances IFNγ-induced iNOS expression, which is suppressed by inhibitors of NF-κB or p38 MAP kinase (Trajkovic et al., 2001). Thus, IL-17 functions as a proinflammatory cytokine that works synergistically with other inflammatory stimuli in the CNS.

In addition to the proinflammatory effects on microglia, IL-17 also enhanced the expression of neurotrophic factors by microglia. We and other groups have previously shown that proinflammatory cytokines or inflammatory stimuli induce the expression of neurotrophic factors in microglia (Suzumura et al., 2006; Bessis et al., 2007). This may contribute to anti-inflammatory defense mechanisms in the CNS and implies that microglia may have multiple functions.

Previous cDNA microarray and immunohistochemical studies have suggested that astrocytes produce IL-17 (Meeuwsen et al., 2003; Li et al., 2005). In this study, we showed for the first time that microglia produce IL-17 in response to IL-23 or IL-1β. Although IL-1β and IL-23 induced IL-17 mRNA expression in microglia, we did not detect IL-17 in the supernatant of these cells. It is possible that IL-1β and IL-23 stimulate microglia to produce very low amount of IL-17 that cannot be detected with a commercially available ELISA kit, or that microglia may require another stimulatory signal before they release IL-17.

The same stimulus, however, did not induce the expression of IL-17 mRNA and protein in astrocytes. Thus, other stimuli may induce astrocytes to produce IL-17. Alternatively, this result may be due to differences between the species. As we and other groups have shown, IL-1β and IL-23 are produced by microglia in the CNS (Sonobe et al., 2005; Suzumura et al., 2006; Li et al., 2007). Therefore, it is possible that IL-1β and IL-23 may function as autocrine mediators that induce IL-17 expression by microglia.

Both Th1 and Th2 cytokines negatively regulate the differentiation of IL-17-producing T cells (Iwakura and Ishigame, 2006). In contrast, recent studies suggest that TGF-β derived from regulatory T cells induces an upregulation of IL-23 receptor expression and differentiation of Th17 cells in the presence of IL-6 (Ivanov et al., 2006; Valdhoen et al., 2006). Neither TGF-β nor IL-6, however, affects IL-17 production in microglia. Treatment of IL-23-stimulated microglia with both TGF-β and IL-6 also failed to enhance IL-17 production. These results suggest that different regulatory mechanisms control IL-17 production in microglia and Th17 cells.

Microglia play a pivotal role in the pathogenesis of inflammatory autoimmune diseases in the CNS. Thus, therapeutic targeting of the microglial production of IL-17 might be a useful strategy to treat MS. Because IL-17 deficiency has been demonstrated to ameliorate EAE in mice (Komiyama et al., 2006), induction of neutralizing antibodies that target the IL-23/IL-17 immune axis in microglia may provide a novel therapeutic approach for the treatment of MS. Indeed, targeting IL-23 with neutralizing antibodies ameliorates EAE and reduces serum levels of IL-17 (Chen et al., 2006). Moreover, a previous study demonstrated that blocking IL-17 with neutralizing antibodies induced by an active vaccination efficiently delays the onset of disease and reduces the severity of EAE (Röhn et al., 2006). Inflammatory autoimmune diseases such as MS, however, are chronic in nature, and treatment of these diseases with autoantibodies is extremely costly. Active

vaccination against IL-17 may therefore be an attractive therapeutic alternative, which could allow more patients access to an effective therapy that acts at an earlier stage of disease.

Acknowledgments

This work was supported in part by a Grant-in-Aid for Scientific Research and for the Creation of Innovations through the Business-Academic-Public Sector Cooperation from the Ministry of Education, Culture, Sports, Science and Technology of Japan as well as a Grant-in-Aid for Medical Frontier Strategy Research and for Research on Intractable Diseases from the Japanese Ministry of Health, Labour and Welfare. This work was also supported by the 21st COE Program "Integrated Molecular Medicine for Neuronal and Neoplastic Disorders" from the Ministry of Education, Culture, Sports, Science and Technology.

References

Aggarwal, S., Gurney, A.L., 2002. IL-17: prototype member of an emerging cytokine family. J. Leukoc. Biol. 71, 1–8.

Aggarwal, S., Ghilardi, N., Xie, M.H., de Sauvage, F.J., Gurney, A.L., 2003. Interleukin-23 promotes a distinct CD4 T cell activation state characterized by the production of interleukin-17. J. Biol. Chem. 278 (3), 1910–1914.

Batten, M., Li, J., Yi, S., Kljavin, N.M., Danilenko, D.M., Lucas, S., Lee, J., de Sauvage, F.J., Ghilardi, N., 2006. Interleukin 27 limits autoimmune encephalomyelitis by suppressing the development of interleukin 17-producing T cells. Nat. Immunol. 7, 929–936.

Bessis, A., Bechade, C., Bernard, D., Roumier, A., 2007. Microglial control of neuronal death and synaptic properties. Glia 55 (3), 233–238 Review.

Bettelli, E., Carrier, Y., Gao, W., Korn, T., Strom, T.B., Oukka, M., Weiner, H.L., Kuchroo, V.K., 2006. Reciprocal developmental pathways for the generation of pathogenic effector TH17 and regulatory T cells. Nature 441 (7090), 235–238.

Cai, X.Y., Gommoll Jr., C.P., Justice, L., Narula, S.K., Fine, J.S., 1998. Regulation of granulocyte colony-stimulating factor gene expression by interleukin-17. Immunol. Lett. 62, 51–58.

Chabaud, M., Fossiez, F., Taupin, J.L., Miossec, P., 1998. Enhancing effect of IL-17 on IL-1-induced IL-6 and leukemia inhibitory factor production by rheumatoid arthritis synoviocytes and its regulation by Th2 cytokines. J. Immunol. 161, 409–414.

Chen, Y., Langrish, C.L., McKenzie, B., Joyce-Shaikh, B., Stumhofer, J.S., McClanahan, T., Blumenschein, W., Churakovsa, T., Low, J., Presta, L., Hunter, C.A., Kastelein, R.A., Cua, D.J., 2006. Anti-IL-23 therapy inhibits multiple inflammatory pathways and ameliorates autoimmune encephalomyelitis. J. Clin. Invest. 116 (5), 1317–1326.

Fossiez, F., Djossou, O., Chomarat, P., Flores-Romo, L., Ait-Yahia, S., Maat, C., Pin, J.J., Garrone, P., Garcia, E., Saeland, S., Blanchard, D., Gaillard, C., Das, M.B., Rouvier, E., Golstein, P., Banchereau, J., Lebecque, S., 1996. T cell interleukin-17 induces stromal cells to produce proinflammatory and hematopoietic cytokines. J. Exp. Med. 183, 2593–2603.

Furukawa, S., Kamo, I., Furukawa, Y., Akazawa, S., Satoyoshi, E., Itoh, K., Hayashi, K., 1983. A highly sensitive enzyme immunoassay for mouse beta nerve growth factor. J. Neurochem. 40, 734–744.

Harrington, L.E., Hatton, R.D., Mangan, P.R., Turner, H., Murphy, T.L., Murphy, K.M., Weaver, C.T., 2005. Interleukin 17-producing $CD4^+$ effector T cells develop via a lineage distinct from the T helper type 1 and 2 lineages. Nat. Immunol. 6 (11), 1123–1132.

Hofstetter, H.H., Ibrahim, S.M., Koczan, D., Kruse, N., Weishaupt, A., Toyka, K.V., Gold, R., 2005. Therapeutic efficacy of IL-17 neutralization in murine experimental autoimmune encephalomyelitis. Cell Immunol. 237 (2), 123–130.

Ignarro, L.J., Buga, G.M., Wood, K.S., Byrns, R.E., Chaudhuri, G., 1987. Endothelium-derived relaxing factor produced and released from artery and vein in nitric oxide. Proc. Natl. Acad. Sci. USA, 84, 9265–9269.

Ishizu, T., Osoegawa, M., Mei, F.J., Kikuchi, H., Tanaka, M., Takakura, Y., Minohara, M., Murai, H., Mihara, F., Taniwaki, T., Kira, J., 2005. Intrathecal activation of the IL-17/IL-8 axis in opticospinal multiple sclerosis. Brain 128, 988–1002.

Ivanov, I.I., McKenzie, B.S., Zhou, L., Tadokoro, C., Lepelley, A., Lafaille, J., Cua, D., Littman, D., 2006. The orphan nuclear receptor RORgammat directs the differentiation program of proinflammatory IL-17^+ T helper cells. Cell 126, 1121–1133.

Iwakura, Y., Ishigame, H., 2006. The IL-23/IL-17 axis in inflammation. J. Clin. Invest. 116 (5), 1218–1922.

Jovanovic, D.V., Di, B.J.A., Martel-Pelletier, J., Jolicoeur, F.C., He, Y., Zhang, M., Mineau, F., Pelletier, J.P., 1998. IL-17 stimulates the production and expression of proinflammatory cytokines, IL-b and TNFa, by human macrophages. J. Immunol. 160, 3513–3521.

Kaechi, K., Furukawa, Y., Ikegami, R., Nakamura, N., Omae, F., Hashimoto, Y., Hayashi, K., Furukawa, S., 1993. Pharmacological induction of physiologically active nerve growth factor in rat peripheral nervous system. J. Pharmacol. Exp. Ther. 264, 321–326.

Kennedy, J., Rossi, D.L., Zurawski, S.M., Vega Jr., F., Kastelein, R.A., Wagner, J.L., Hannum, C.H., Zlotnik, A., 1996. Mouse IL-17: a cytokine preferentially expressed by alpha beta TCR+$CD4^-CD8^-$T cells. J. Interferon Cytokine Res. 16, 611–617.

Komiyama, Y., Nakae, S., Matsuki, T., Nambu, A., Ishigame, H., Kakuta, S., Sudo, K., Iwakura, Y., 2006. IL-17 plays an important role in the development of experimental autoimmune encephalomyelitis. J. Immunol. 177, 566–573.

Kuno, R., Yoshida, Y., Nitta, A., Nabeshima, T., Wang, J., Sonobe, Y., Kawanokuchi, J., Takeuchi, H., Mizuno, T., Suzumura, A., 2006. The role of TNF-alpha and its receptors in the production of NGF and GDNF by astrocytes. Brain Res. 1116 (1), 12–18.

Laan, M., Cui, Z.H., Hoshino, H., Lotvall, J., Sjostrand, M., Gruenert, D.C., Skoogh, B.E., Linden, A., 1999. Neutrophil recruitment by human IL-17 via C–X–C chemokine release in the airways. J. Immunol. 162, 2347–2352.

Laemmli, U.K., Favre, M., 1973. Maturation of the head of bacteriophage T4. I. DNA packaging events. J. Mol. Biol. 80 (4), 575–579.

Li, G.Z., Zhong, D., Yang, L.M., Sun, B., Zhong, Z.H., Yin, Y.H., Cheng, J., Yan, B.B., Li, H.L., 2005. Expression of interleukin-17 in ischemic brain tissue. Scand. J. Immunol. 62 (5), 481–486.

Li, Y., Chu, N., Hu, A., Gran, B., Rostami, A., Zhang, G.X., 2007. Increased IL-23p19 expression in multiple sclerosis lesions and its induction in microglia. Brain 130 (Pt2), 490–501.

Linden, A., Hoshino, H., Laan, M., 2000. Airway neutrophils and interleukin-17. Eur. Respir. J. 15, 973–977.

Lock, C., Hermans, G., Pedotti, R., Brendolan, A., Schadt, E., Garren, H., Langer-Gould, A., Strober, S., Cannella, B., Allard, J., Klonowski, P., Austin, A., Lad, N., Kaminski, N., Galli, S.J., Oksenberg, J.R., Raine, C.S., Heller, R., Steinman, L., 2003. Gene-microarray analysis of multiple sclerosis lesions yields new targets validated in autoimmune encephalomyelitis. Nat. Med. 8 (5), 500–208.

Matusevicius, D., Kivisakk, P., He, B., Kostulas, N., Ozenci, V., Fredrikson, S., Link, H., 1999. Interleukin-17 mRNA expression in blood and CSF mononuclear cells is augmented in multiple sclerosis. Mult. Scler. 5 (2), 101–104.

Meeuwsen, S., Persoon-Deen, C., Bsibsi, M., Ravid, R., van Noort, J.M., 2003. Cytokine, chemokine and growth factor gene profiling of cultured human astrocytes after exposure to proinflammatory stimuli. Glia 43 (3), 243–253.

Nitta, A., Ito, M., Fukumitsu, H., Ohmiya, M., Ito, H., Sometani, A., Nomoto, H., Furukawa, Y., Furukawa, S., 1999. 4-methylcatechol increases brain-derived neurotrophic factor content and mRNA expression in cultured brain cells and in rat brain in vivo. J. Pharmacol. Exp. Ther. 291, 1276–1283.

Nitta, A., Nishioka, H., Fukumitsu, H., Furukawa, Y., Sugiura, H., Shen, L., Furukawa, S., 2004. Hydrophobic dipeptide Leu-Ile protects against neuronal death by inducing brain-derived neurotrophic factor and glial cell line-derived neurotrophic factor synthesis. J. Neurosci. Res. 78, 250–258.

Park, H., Li, Z., Yang, X.O., Chang, S.H., Nurieva, R., Wang, Y.H., Wang, Y., Hood, L., Zhu, Z., Tian, Q., Dong, C., 2005. A distinct lineage of CD4 T cells regulates tissue inflammation by producing interleukin 17. Nat. Immunol. 6 (11), 1133–1141.

Pollock, J.S., Forstermann, U., Mitchell, J.A., Warner, T.D., Schmidt, H.H.H.W., Nakane, M., Murad, F., 1991. Purification and characterization of particulate endothelium-derived relaxing factor synthase from cultured and native bovine aortic endothelial cells. Proc. Natl. Acad. Sci. 88, 10480–10484.

Röhn, T.A., Jennings, G.T., Hernandez, M., Grest, P., Beck, M., Zou, Y., Kopf, M., Bachmann, M.F., 2006. Vaccination against IL-17 suppresses autoimmune arthritis and encephalomyelitis. Eur. J. Immunol. 36 (11), 2844–2848.

Sonobe, Y., Yawata, I., Kawanokuchi, J., Takeuchi, H., Mizuno, T., Suzumura, A., 2005. Production of IL-27 and other IL-12 family cytokines by microglia and their subpopulations. Brain Res. 1040 (1–2), 202–207.

Suzumura, A., Mezitis, S.G., Gonatas, N.K., Silberberg, D.H., 1987. MHC antigen expression on bulk isolated macrophage-microglia from newborn mouse brain: induction of Ia antigen expression by gamma-interferon. J. Neuroimmunol. 15 (3), 263–278.

Suzumura, A., Takeuchi, H., Zhang, G., Kuno, R., Mizuno, T., 2006. Roles of glia-derived cytokines on neuronal degeneration and regeneration. Ann. N. Y. Acad. Sci. 1088, 219–229 Review.

Takeuchi, H., Mizuno, T., Zhang, G., Wang, J., Kawanokuchi, J., Kuno, R., Suzumura, A., 2005. Neuritic beading induced by activated microglia is an early feature of neuronal dysfunction toward neuronal death by inhibition of mitochondrial respiration and axonal transport. J. Biol. Chem. 280 (11), 10444–10454.

Towbin, H., Staehelin, T., Gordon, J., 1979. Electrophoretic transfer of proteins from polyacrylamide gels to nitrocellulose sheets: procedure and some applications. Proc. Natl. Acad. Sci. U. S. A. 76 (9), 4350–4354.

Trajkovic, V., Stosic-Grujicic, S., Samardzic, T., Markovic, M., Miljkovic, D., Ramic, Z., MostaricaStojkovic, M., 2001. Interleukin-17 stimulates inducible nitric oxide synthase activation in rodent astrocytes. J. Neuroimmunol. 119, 183–191.

Valdhoen, M., Hocking, R.J., Atkins, C.J., Locksley, R.M., Stockinger, B., 2006. TGFbeta in the context of an inflammatory cytokine milieu supports de novo differentiation of IL-17 producing T cells. Immunity 24, 179–189.

Yao, Z., Painter, S.L., Fanslow, W.C., Ulrich, D., Macduff, B.M., Spriggs, M.K., Armitage, R.J., 1995. Human IL-17: a novel cytokine derived from T cells. J. Immunol. 155 (12), 5483–5486.

0022-3565/08/3271-137–147$20.00
THE JOURNAL OF PHARMACOLOGY AND EXPERIMENTAL THERAPEUTICS
Copyright © 2008 by The American Society for Pharmacology and Experimental Therapeutics
JPET 327:137–147, 2008

Vol. 327, No. 1
141309/3384925
Printed in U.S.A.

The Extensive Nitration of Neurofilament Light Chain in the Hippocampus Is Associated with the Cognitive Impairment Induced by Amyloid β in Mice

Tursun Alkam, Atsumi Nitta, Hiroyuki Mizoguchi, Akio Itoh, Rina Murai, Taku Nagai, Kiyofumi Yamada, and Toshitaka Nabeshima

Department of Neuropsychopharmacology and Hospital Pharmacy, Nagoya University Graduate School of Medicine, Nagoya, Japan (T.A., A.N., H.M., A.I., R.M., T.Nag., K.Y., T.Nab.); Department of Basic Medicine, College of Traditional Uighur Medicine, Hotan, China (T.A.); and Department of Chemical Pharmacology, Graduate School of Pharmaceutical Science, Meijo University, Nagoya, Japan (T.Nab.)

Received May 19, 2008; accepted July 9, 2008

ABSTRACT

Tyrosine nitration of proteins at an extensive level is widely associated with the cognitive pathology induced by amyloid β peptide (Aβ). However, the precise identity and explicit consequences of protein nitration have scarcely been addressed. In this study, we examined the detectable nitration of proteins in the hippocampus of mice with cognitive impairment (day 5) induced by the i.c.v. injection of $A\beta_{25-35}$ (day 0). The intensity of the nitration of proteins was inversely associated with the level of recognition memory in mice. The detectable tyrosine nitrations were revealed in proteins with a single size of approximately 70 kDa. The specific nitrated proteins at this size were identified using the liquid chromatography/mass spectrometry/mass spectrometry analysis and immunodetection methods. Intense nitration of the neurofilament light chain (NFL) was observed. The increased nitration of NFL was associated with its serine hyperphosphorylation and weak interaction with the nuclear distribution element-like, a protein essential for the stable assembly of neurofilaments. No changes in cell numbers in the hippocampus were found (day 5) in mice that received $A\beta_{25-35}$ injections. These findings suggested that extensive nitration of NFL is associated with the Aβ-induced impairment of recognition memory in mice.

Increased nitration of proteins, a surrogate marker of widespread oxidative damage in brains affected by the amyloid β peptide (Aβ), is evidently correlated with the severity of cognitive dysfunction in humans as well as animals (Smith et al., 1997; Lim at al., 2001; Perry et al., 2002; Kim et al., 2003; Andersen, 2004; Bastianetto and Quirion, 2004; Walsh and Selkoe, 2004).

We have previously reported the contribution of tyrosine nitration to Aβ-induced, oxidative damage-mediated cognitive dysfunction in mice (Alkam et al., 2007, 2008). A mouse monoclonal anti-nitrotyrosine antibody in Western blot analysis identified the tyrosine-nitrated hippocampal proteins at approximately 70 kDa as a single band with which the severity of cognitive impairments in mice was well associated (Alkam et al., 2007). In this study, we aimed to identify the nitrated proteins in the single band for the specification of the contribution of the extensive nitration of tyrosine to the cognitive impairment. To produce strong and stable nitrative damage, we applied $A\beta_{25-35}$, a toxic Aβ fragment that is detected in the human brain (Pike et al., 1995; Kubo et al., 2002). The tyrosine-nitrated proteins were examined by using liquid chromatography/mass spectrometry/mass spec-

This work was supported, in part, by the following: Japan-China Sasakawa Medical fellowship (to T.A.); Uehara Memorial Foundation fellowship for Foreign Researchers in Japan (to T.A.); grant-in-aid for the 21st Century Center of Excellence Program "Integrated Molecular Medicine for Neuronal and Neoplastic Disorders" and "Academic Frontier Project for Private Universities (2007–2011)" from the Ministry of Education, Culture, Sports, Science and Technology of Japan; Comprehensive Research on Aging and Health from the Ministry of Health, Labor and Welfare of Japan; Japan-Canada Joint Health Research Program and Japan-France Joint Health Research Program (Joint Project from Japan Society for the Promotion of Science); and International Research Project Supported by the Meijo Asian Research Center.

Article, publication date, and citation information can be found at http://jpet.aspetjournals.org.

doi:10.1124/jpet.108.141309.

ABBREVIATIONS: Aβ, amyloid β peptide; LC-MS/MS, liquid chromatography/mass spectrometry/mass spectrometry; NFL, neurofilament light chain; NUDEL, nuclear distribution element-like; NF, neurofilament; $ONOO^-$, peroxynitrite; UA, uric acid; RIPA, radioimmunoprecipitation assay; PBS, phosphate-buffered saline; PAGE, polyacrylamide gel electrophoresis; PVDF, polyvinylidene difluoride; HSP70, heat shock protein 70; DRP-2, dihydropyrimidinase-like 2; GAPDH, glyceraldehyde 3-phosphate dehydrogenase; SD, sodium dithionite; CBB, Coomassie Brilliant Blue; AD, Alzheimer's disease.

trometry (LC-MS/MS) and immunodetection. Intense nitration of the neurofilament light chain (NFL) was observed. The intensive nitration was associated with serine hyperphosphorylation and reduced interaction of NFL with nuclear distribution element-like (NUDEL), a protein essential for the stable assembly of neurofilaments (NFs). The results provided further support for the conception that extensive nitration of tyrosine in proteins underlies one of the key mechanisms contributing to the cognitive pathology induced by Aβ.

Materials and Methods

Animals. Male ICR mice (Nihon SLC Co., Shizuoka, Japan) were used. The animals were housed in a controlled environment (23 ± 1°C, 50 ± 5% humidity) and allowed access to food and water ad libitum. The room lights were kept on between 8:00 AM and 8:00 PM. All experiments were performed in accordance with the Guidelines for Animal Experiments of Nagoya University Graduate School of Medicine. The procedures involving animals and their care conformed to the *Guidelines for Proper Conduct of Animal Experiments* (Science Council of Japan, 2006).

Treatment and Experimental Design. $A\beta_{25-35}$ (Bachem, Bubendorf, Switzerland) was dissolved in sterile double-distilled water to a stock concentration of 1 mg/ml and stored at −20°C before use. The dissolved $A\beta_{25-35}$ was incubated for aggregation at 37°C for 4 days. The distilled water was incubated at the same conditions and used as the vehicle. $A\beta_{1-40}$ (Bachem) was dissolved to a stock concentration of 1.0 mg/ml in 35% acetonitrile/0.1% trifluoroacetic acid and stored at −20°C before use. The solution of peroxynitrite ($ONOO^-$; 144 mM) (Millipore, Billerica, MA) was stored at −80°C before use. Incubated $A\beta_{25-35}$ (3 μg/3 μl), incubated distilled water (3 μl), $A\beta_{1-40}$ (5 μg/5 μl), and $ONOO^-$ (144 mM/1 μl) were administered by i.c.v. injection as described previously (Maurice et al., 1996; Alkam et al., 2007, 2008). In brief, a microsyringe with a 28-gauge stainless steel needle 3.0-mm long was used for all experiments. Mice were anesthetized lightly with ether, and the needle was inserted unilaterally 1 mm to the right of the midline point equidistant from each eye, at an equal distance between the eyes and the ears and perpendicular to the plane of the skull. A single shot of the indicated volume of agents was delivered gradually within 3 s. Mice exhibited normal behavior within 1 min after the injection. The injection placement or needle track was visible and was verified at the time of dissection. Neither insertion of the needle nor the volume of injection had a significant influence on survival, behavioral responses, or cognitive functions. Uric acid (UA) (Wako Pure Chemicals, Osaka, Japan) was prepared as a suspension in saline. Immediately after the single injection of $A\beta_{25-35}$ or $A\beta_{1-40}$, mice were given UA (100 mg/kg i.p.) daily for 6 consecutive days. The schedule of administration of peptides and drugs as well as biochemical, histochemical, and behavioral investigations is shown in Fig. 1.

Novel Object Recognition Task. This task, based on the spontaneous tendency of rodents to explore a novel object more often than a familiar one, was performed on days 3 to 5 after the i.c.v. injection of $A\beta_{1-40}$, $A\beta_{25-35}$, or peroxynitrite (day 0) as described previously (Alkam et al., 2007). A plastic chamber (35 × 35 × 35 cm) was used in low light conditions during the light phase of the light/dark cycle. The general procedure consisted of three different phases: 1) a habituation phase, 2) an acquisition phase, and 3) a retention phase. On the 1st day (habituation phase), mice were individually subjected to a single familiarization session of 10 min, during which time they were introduced into the empty arena to become familiar with the apparatus. On the 2nd day (acquisition phase), the animals were subjected to a single 10-min session, during which time two floor-fixed objects (A and B) were placed in a symmetric position from the center of the arena, 15 cm from each other and 8 cm from the nearest wall. The two objects, made of the same wooden material with a similar color and smell, were different in shape but identical in size. Mice were allowed to explore the objects in the open field. A preference index for each mouse was expressed as a ratio of the amount of time spent exploring object A (TA × 100)/(TA + TB), where TA and TB are the time spent exploring object A and object B, respectively. On the 3rd day (retention phase), mice were allowed to explore the open field in the presence of two objects: the familiar object A and a novel object C in different shapes but in similar color and size (A and C). A recognition index, calculated for each mouse, was expressed as the ratio (TC × 100)/(TA + TC), where TA and TC are the time spent during the retention phase on object A and object C, respectively. The time spent exploring the object (nose pointing toward the object at a distance ≤ 1 cm) was recorded by hand.

Sample Preparation. Animals were decapitated, and the hippocampi were removed on an ice-cold glass plate and stored at −80°C. Hippocampal protein extracts were obtained by homogenization in diverse ice-cold lysis buffers that included the radioimmunoprecipitation assay (RIPA) buffer, phosphate-buffered saline (PBS) buffer, Triton X-100 buffer, and 6 M urea buffer. The RIPA lysis buffer contained 20 mM trizma hydrochloride, pH 7.6, 150 mM sodium chloride, 2 mM EDTA·2Na, 50 mM sodium fluoride, 1 mM sodium vanadate, 1% Nonidet P-40, 1% sodium deoxycholate, 0.1% SDS, 1 mg/ml pepstatin, 1 mg/ml aprotinin, and 1 mg/ml leupeptin. The PBS lysis buffer, pH 7.4, contained 135 mM sodium chloride, 3.2 mM disodium hydrogen phosphate 12-water, 1.3 mM potassium chloride, and 0.5 mM potassium dihydrogen phosphate. The Triton X-100 buffer contained 10 mM trizma hydrochloride at pH 7.5, 150 mM sodium chloride, 1 mM EDTA at pH 8.0, and 1% Triton X-100. The 6 M urea lysis buffer contained 10 mM trizma base at pH 8.1, 6 M urea, and 1 mM dithiothreitol. All of these lysis buffers, with the exception of the RIPA buffer, were supplemented with complete protease inhibitor cocktail tablets (Roche Applied Science, Mannheim, Germany). Homogenates were centrifuged at 13000*g* for 20 min to obtain the desired supernatant of the extracts. The centrifuged pellets were washed twice with the previous buffer before being solubilized. The washing procedure consisted of complete dispersion of the pellets by vortexing and incubation in ice for 30 min followed by centrifugation at 13000*g* for 20 min. The unassembled NFL and NUDEL proteins were obtained within the soluble proteins in Triton X-100 buffer (Nguyen et al., 2004), and the insoluble protein pellets that include the assembled NFL and NUDEL proteins were then solubilized in 6 M urea lysis buffer (Crow et al., 1997). The cytoplasmic water-soluble proteins were obtained in PBS lysis buffer (Aoyama and Kitajima, 1999), and the insoluble pellets were then solubilized in Triton X-100 buffer. The concentrations of PBS-soluble and urea-soluble proteins were determined with a Bio-Rad protein assay reagent kit (Bio-Rad, Hercules, CA). The concentrations of the Triton

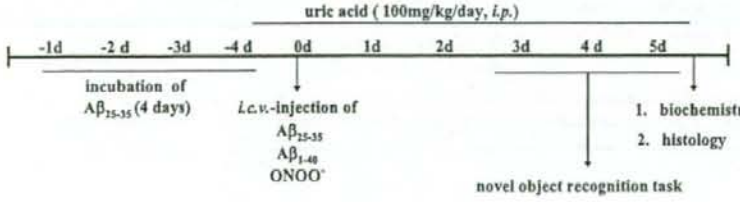

Fig. 1. The experimental design of the study.

X-100-soluble proteins were determined with a BCA protein assay reagent kit (Pierce, Rockford, IL).

Western Blot Analysis. Equal amounts (20 μg) of protein sample were resolved by a 4 to 20% gradient or 7% SDS-polyacrylamide gel electrophoresis (PAGE). The proteins were then transferred electrophoretically to a polyvinylidene difluoride (PVDF) membrane (Millipore). Membranes were incubated in 3% skim milk or 3% bovine serum albumin (for phosphor-protein) in phosphate-buffered saline containing 0.05% (v/v) Tween 20 for 2 h at room temperature. Anti-nitrotyrosine mouse monoclonal 1A6 antibody (catalog number 05-233; Millipore), anti-NFL mouse antibody (Sigma-Aldrich, St. Louis, MO), anti-heat shock protein 70 (HSP70) polyclonal antibody (Assay Designs, Ann Arbor, MI), anti-dihydropyrimidinase-like 2 (DRP-2) mouse antibody (IBL, Takasaki, Japan), anti-NUDEL rabbit antibody (Abcam Inc., Cambridge, MA), anti-phosphoserine rabbit antibody (Zymed Laboratories, South San Francisco, CA), anti-β-actin goat antibody (Santa Cruz Biotechnology Inc., Santa Crutz, CA), and anti-glyceraldehyde 3-phosphate dehydrogenase (GAPDH) mouse antibody (Imgenex, San Diego, CA) were used. To confirm the specificity of the detected single band of tyrosine-nitrated proteins, the reduction of nitrotyrosine to aminotyrosine was performed. In brief, the membrane was treated with 10 mM sodium dithionite (SD) in 50 mM pyridine-acetate buffer, pH 5.0, for 1 h at room temperature. After the reaction, the membrane was rinsed with distilled water and then equilibrated with washing buffer and blocked for 1 h at room temperature in blocking solution before standard procedures of Western blotting were followed. The absent band in the SD-treated membrane compared with the routine-treated control membrane was regarded to be a genuine for nitrated proteins. To confirm the specificity of the detected band for phosphoserine, the anti-phosphoserine inhibitor (the inhibitor) that contains phosphoserine was used to block the specific interaction of anti-phosphoserine primary antibodies with serine-phosphorylated proteins in the membrane. In brief, the anti-phosphoserine primary antibody and the inhibitor at a final concentration of 20 mM were mixed into a bovine serum albumin-containing blocking buffer and preincubated for 10 min for the ample binding of the antibodies with the phosphoserines (to cover up all of the specific anti-phosphoserine antibodies) before the application to the membrane. Incubation of the antibody-inhibitor mixture with the membrane was carried out for 1 h at room temperature. After the incubation, standard procedures were followed for blot washing and incubation with a secondary antibody. The absence of the bands in the membrane after the antibody-inhibitor treatment compared with the membrane subjected to routine treatment was regarded as genuine proof of serine phosphorylation. The intensity of each protein band on the film was analyzed with the Atto Densitograph 4.1 system (Atto, Tokyo, Japan) and was corrected with the corresponding β-actin or GAPDH level. The results were expressed as a percentage of that in the naive group.

Liquid Chromatography/Mass Spectrometry/Mass Spectrometry. Protein bands in the SDS-PAGE were stained with Coomassie Brilliant Blue (CBB) (Fluka, Buchs, Switzerland). The band of interest was excised from the gel. The gel piece was digested in trypsin solution at 35°C for 20 h for analysis by LC/MS/MS (Aproscience Lifescience Institute, Tokushima, Japan).

Immunoprecipitation. Hippocampal homogenates for Western blottings were used for immunoprecipitation. The antibodies against the proteins of interest were incubated overnight with 50 μl of protein A-Sepharose beads (GE Healthcare, Little Chalfont, Buckinghamshire, UK). To obtain tyrosine-nitrated proteins, anti-nitrotyrosine agarose-conjugated mouse antibody (Millipore) was used. The bead-antibody complexes were incubated overnight with 500 μg of precleared proteins in the corresponding buffers, with the exception that urea lysis buffer does not include dithiothreitol. Immunocomplexes were collected by centrifugation at 13000*g* for 1 min at 4°C and then washed three times with ice-cold PBS. Immunoprecipitated samples were recovered by resuspending in 2× sample loading buffer, immediately fractionated by reducing in 7% SDS-PAGE, and analyzed by Western blotting with the corresponding antibodies.

Histology. Each mouse was anesthetized with diethyl ether and quickly intracardially perfused with physiological saline followed by 4% paraformaldehyde in 100 mM PBS, pH 7.4. The brains were quickly removed, postfixed for 24 h in the same fixative solution, and cryoprotected in a graded 10 to 40% sucrose solution in 100 mM PBS. Coronal sections were cut 20-μm thick using a cryostat (Leica, Wetzlar, Germany) and stained with 0.1% cresyl violet reagent (Wako Pure Chemicals) according to standard procedures. The sections were mounted in fluorescent medium (Dako North America, Inc., Carpinteria, CA), and images of CA1, CA3, and the granular layer of the dentate gyrus of the hippocampus were taken using a Carl Zeiss Axioskop phase-contrast microscope with a cooled CCD camera system (SenSys; Photometrics Ltd., Tucson, AZ). The Nissl-positive neuronal cells were counted using Image J software (version 1.38; National Institutes of Health, Bethesda, MD). The total cell count in per millimeter square was averaged from four sections per animal ($n = 4$) according to previous reports (Nabeshima et al., 1991; Nitta et al., 1997).

Statistical Analysis. The results are expressed as the mean ± S.E. Statistical significance was determined with a one-way analysis of variance followed by the Bonferroni multiple comparisons test. $p < 0.05$ was taken as a significant level of difference.

Results

The Tyrosine Nitration of Proteins Induced by $A\beta_{25-35}$ in the Hippocampus of Mice. Anti-nitrotyrosine mouse antibody detected only a single band of hippocampal proteins at approximately 70 kDa for tyrosine nitration, which induced a potent nitrating agent after the i.c.v. injection of $A\beta_{1-40}$, $A\beta_{25-35}$, and peroxynitrite ($ONOO^-$) (Fig. 2A). Aβ peptides induced extensive nitration of proteins in the hippocampus and impairment of recognition memory, both of which were prevented by UA, a potent scavenger of $ONOO^-$. $ONOO^-$ induced marked tyrosine nitration of proteins in the hippocampus and impairment of recognition memory (Fig. 2, B and C). The intensity of the nitration was inversely associated with the recognition memory in mice (Fig. 2D). The authenticity of nitration was confirmed by the reduction of nitrotyrosine to aminotyrosine with SD in the membrane and by detecting the nitrotyrosine using the same antibody. The absence of this band after SD treatment was regarded as a genuine band for proteins with tyrosine nitration (Fig. 2, E and F). Proteins in SDS-PAGE were stained with CBB, and the 70-kDA protein band was excised for identification (Fig. 2G). The proteins in the excised gel were in-gel-trypsin-digested and subjected to LC/MS/MS, and several proteins were successfully identified (Table 1).

The Identification of the Tyrosine-Nitrated Proteins and the Level of Nitration. The nitration of the identified proteins was examined by applying the immunoprecipitation method. For peptide match scores, HSP70, DRP-2, and NFL were favored for the further study. Because the antibody that was used to detect the nitrated proteins in Western blot analysis could not be used for immunoprecipitation, a specially designed agarose-conjugated mouse anti-nitrotyrosine monoclonal antibody was used. We applied $A\beta_{25-35}$ for the rest of the study, considering its property to produce stronger and stable oxidative damage (Pike et al., 1995) as evidenced in Fig. 2. Immunoprecipitated nitrated-proteins were fractionated by SDS-PAGE and blotted with the antibodies raised against the proteins of interest (Fig. 3A). Intensive

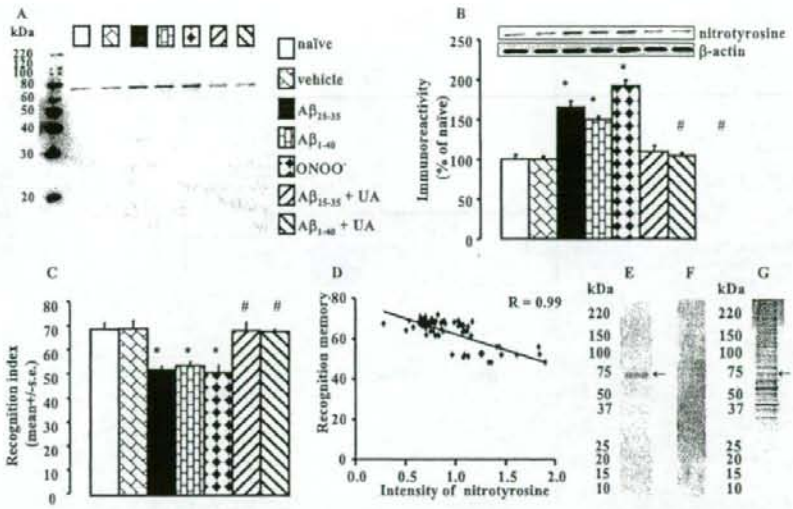

Fig. 2. The tyrosine nitration of proteins in the hippocampus and the cognitive function in mice. A and B, nitrotyrosine in the hippocampus was measured 5 days after the i.c.v. injection of Aβ peptides or $ONOO^-$. Protein samples from the hippocampus were subjected to SDS-PAGE, blotted to a PVDF membrane, and probed with a monoclonal anti-nitrotyrosine antibody. Aβ peptides induced extensive nitration of protein, which was prevented by UA, a potent scavenger of $ONOO^-$. $ONOO^-$ induced marked tyrosine nitration of proteins. The quantified intensity of the bands for nitrotyrosine was corrected by that of β-actin and expressed as a percentage of that in the naive group. Data are presented as the mean ± S.E. (n = 4). *, $p < 0.05$ versus naive and vehicle; #, $p < 0.05$ versus $A\beta_{25-35}$ or $A\beta_{1-40}$. C, the novel object recognition task was performed on days 3 to 5 after the i.c.v. injection of Aβ peptides or $ONOO^-$. Aβ peptides induced marked impairments of recognition memory, which were prevented by UA. $ONOO^-$ induced impairment of recognition memory. Data are presented as the mean ± S.E. (n = 10). *, $p < 0.05$ versus naive and vehicle; #, $p < 0.05$ versus $A\beta_{25-35}$ and $A\beta_{1-40}$. D, the panel shows the inverse association of extensive nitration of protein tyrosine in the hippocampus and the level of recognition memory in mice. E and F, protein samples from the hippocampus were subjected to 4 to 20% SDS-PAGE, blotted to PVDF membrane, and probed with a monoclonal anti-nitrotyrosine antibody before (E) and after (F) reduction of nitrotyrosine to aminotyrosine by treating the membrane with SD. G, protein bands in 4 to 20% SDS-PAGE were stained by CBB, and the band of interest was picked up for peptide analysis using LC-MS/MS.

TABLE 1
The identified protein candidates

Protein Name	gi Accession Number	Peptide Matched	% Sequence Coverage	Total Score
HSP70	gi 1661134	22	39	724
DRP-2	gi 40254595	7	20	292
NFL	gi 200038	4	9	254
ATPase, H^+transporting, V1 subunit A, isoform 1	gi 315607	9	17	184
Glycerol-3-phosphate dehydrogenase	gi 1339938	1	2	96
Ig superfamily receptor PGRL	gi 15593237	1	3	55
Solute carrier family 25 (mitochondrial carrier, aralar member12)	gi 27369581	3	8	53

gi, genInfo identifier; PGRL, prostaglandin regulatory-like protein.

nitration was observed for NFL in the $A\beta_{25-35}$ group compared with the naive or vehicle group (Fig. 3, A and B). No differences were observed in the nitration of HSP70 and DRP-2 proteins among the three groups (Fig. 3, A, C, and D). The increased nitration of NFL was inversely associated with recognition memory in mice that received $A\beta_{25-35}$ injections (Fig. 3E).

Association between Extensive Nitration of NFL and Serine Hyperphosphorylation. Hyperphosphorylation of the serine residues of NFL could lead to disruption of the subtle regulation of the NF network (Hisanaga et al., 1990; Nixon and Shea, 1992). After being nitrated in vitro, NFL is not able to form the NF assembly (Crow et al., 1997). The question of whether extensive nitration of NFL influences serine phosphorylation of the protein stimulated our interest. We immunoprecipitated NFL and blotted against nitrotyrosine and phosphoserine. Equal amounts of NFL protein were immunoprecipitated in each group (Fig. 4, A and B). The intensity of the tyrosine nitration and serine phosphorylation of NFL was greater in the $A\beta_{25-35}$ group than in the naive or vehicle group (Fig. 4, A, C, and D). The authenticity of the phosphoserine band was confirmed as indicated under *Materials and Methods*. Treatment with UA prevented the $A\beta_{25-35}$-induced intensive tyrosine nitration and serine hyperphosphorylation of NFL (Fig. 4, A, C, and D), indicating a positive association between the extensive nitration of NFL and the serine hyperphosphorylation (Fig. 4E).

Association between Extensive Nitration of NFL and Its Reduced Interaction with NUDEL. To examine whether the extensive nitration of NFL practically influences its interaction with partner proteins, we focused on the free, unassembled NFL that could be differentiated from the assembled NFL. The majority of the newly synthesized unassembled NF proteins, including NFL, are Triton X-100-solu-

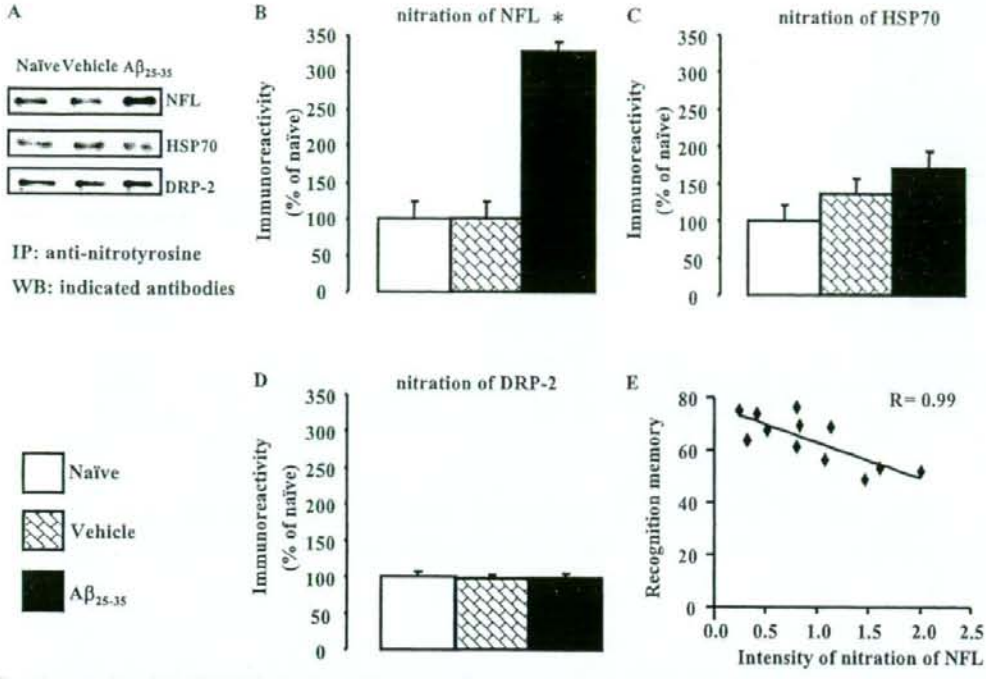

Fig. 3. Tyrosine nitration of the identified proteins. A, immunocomplexes, obtained from precleared protein samples of the hippocampus using an anti-nitrotyrosine agarose-conjugated mouse antibody, were separated by 7% SDS-PAGE, blotted onto a PVDF membrane, and probed with corresponding antibodies raised against the proteins of interest. B to D, NFL was intensely nitrated in the $A\beta_{25-35}$ group, whereas HSP70 and DRP-2 remained unchanged. E, the panel shows inverse association of the extensive nitration of NFL in the hippocampus (B) and the level of recognition memory in mice (Fig. 1B). The intensity of bands was quantified and expressed as a percentage of that in the naive group. Data are presented as the mean ± S.E. (n = 4). *, $p < 0.05$ versus naive and vehicle.

ble before being incorporated into the NF assembly, which is Triton X-100-insoluble (Black et al., 1986). NFL constitutes the core of the NF network, and without NFL, no filaments are formed (Zhu et al., 1997). Without binding directly with NUDEL, the Triton X-100-soluble NFL can barely lead the assembly of a stable NF network, regardless of its own abundance (Nguyen et al., 2004). We probed equal amounts of NFL immunocomplexes with antibodies raised against the nitrotyrosine and NUDEL (Fig. 5, A and B). Less NUDEL was coimmunoprecipitated in the $A\beta_{25-35}$ group that bears extensively nitrated NFL (Fig. 5, A–D). The protein expression of NUDEL did not differ among the groups (Fig. 5E). UA prevented the $A\beta_{25-35}$-induced increase of NFL nitration as well as the reduced coimmunoprecipitation of NUDEL (Fig. 5, A, C, and D). The extensive nitration of NFL was associated with its reduced interaction with NUDEL (Fig. 5F). These results suggested that the intensive nitration of NFL could disturb the normal function of the protein.

Association between Extensive Nitration of NFL and the Reduced Content of NUDEL in the Cytoskeleton Fraction. A majority of NF proteins, after their synthesis in the cytoplasm, are rapidly converted to a Triton X-100-insoluble filamentous network and move down the axon using the transport machinery (Nixon and Shea, 1992). After direct and specific binding with NFL, NUDEL facilitates the assembly of a stable NF network and remains bound to the assembled filaments (Nguyen et al., 2004). Thus, the level of interaction between NFL and NUDEL in cytoplasm (Triton X-100-soluble fraction) should be reflected by their protein levels in the axonal cytoskeleton (Triton X-100-insoluble fraction). The Triton X-100-insoluble fractions from the previous step (Fig. 5) were washed twice with Triton X-100 lysis buffer before being solubilized in urea lysis buffer. Western blot analysis revealed that the level of NUDEL protein was reduced in the $A\beta_{25-35}$ group compared with the naive and vehicle groups, whereas the treatment with UA prevented the reduction (Fig. 6, A and D). This was consistent with the reduced interaction between NFL and NUDEL in the $A\beta_{25-35}$ group (Fig. 5, A and D). However, the level of NFL in the $A\beta_{25-35}$ group was surprisingly not different from that in the naive and vehicle groups (Fig. 6, A and B). Considering the increase of the intensity of the protein nitration in the $A\beta_{25-35}$ group (Fig. 6, A and C), we examined the nitration of NFL by immunoprecipitation. Intense nitration for the NFL protein in the $A\beta_{25-35}$ group was observed (Fig. 6E). Applying the multiplicative inverse (in which the inverse or reciprocal of "n" is "1/n"), a mathematical method that is useful in medical science (Silberberg, 1990), the reciprocal level of the extensively nitrated NFL in the Triton X-100-insoluble fraction was estimated (Fig. 6F). The reciprocal level of extensively nitrated NFL in the $A\beta_{25-35}$ group paralleled with that of NUDEL in the same group (Fig. 6, D and F), signifying a negative effect of the extensive nitration of NFL on NUDEL-dependent NF assembly. The increased nitration of tyrosine could modify protein function by altering the three-dimensional conformation and hydrophobicity (Dalle-Donne et al.,

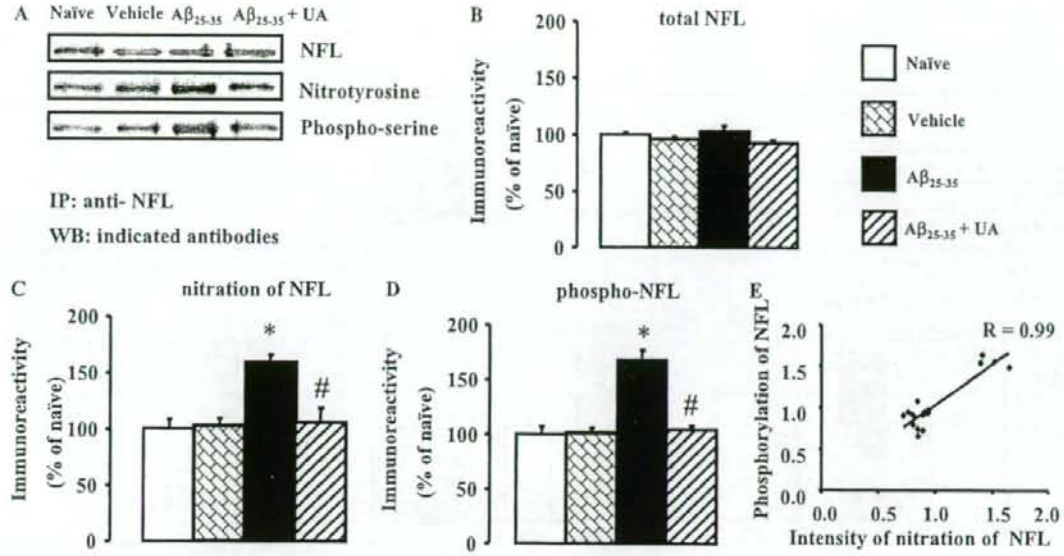

Fig. 4. The association between the increased tyrosine nitration and serine hyperphosphorylation of NFL. A, equal amounts of NFL protein immunocomplexes were obtained from precleared protein samples of the hippocampus, using anti-NFL antibody. The immunocomplexes were separated on SDS-PAGE, blotted onto a PVDF membrane, and probed with the indicated antibodies. B to D, tyrosine nitration and serine phosphorylation of NFL were increased in the $A\beta_{25-35}$ group, whereas UA prevented the increase of both. E, the increased nitration of NFL was correlated with serine hyperphosphorylation of NFL. The intensity of bands was quantified and expressed as a percentage of that in the naive group. Data are presented as the mean ± S.E. ($n = 4$). *, $p < 0.05$ versus naive and vehicle; #, $p < 0.05$ versus $A\beta_{25-35}$.

2005; Reynolds et al., 2007). It was therefore assumed that the overnitrated, free NFL would become less Triton X-100 soluble and, as a result, would be detected in the Triton X-100-insoluble fraction along with the assembled NF proteins. It is hardly practical to separate the unassembled extensively nitrated NFL from the assembled NFL in the Triton X-100-insoluble fraction. The majority of the cytoplasmic water-soluble proteins could be separated from the Triton X-100-soluble protein pools by using PBS lysis buffer in the first step (Aoyama and Kitajima, 1999). After the separation of the PBS-soluble and Triton X-100-soluble proteins as described under *Materials and Methods*, we examined the amount of NFL protein in these two different fractions. The majority of NFL protein in all groups was found in the PBS-soluble cytoplasmic fraction as indicated by GADPH, a cytoplasmic marker (Fig. 7A). The levels of NFL protein in both the PBS-soluble and Triton X-100-soluble fractions were increased in the $A\beta_{25-35}$ group (Fig. 7, A–C). It is interesting to note that the increase of NFL in both fractions was prevented by the treatment with of UA, a potent scavenger of $ONOO^-$, suggesting that the $A\beta_{25-35}$-induced $ONOO^-$ may increase the protein synthesis of NFL before extensively nitrating the protein (Fig. 7, A–C). The Triton X-100-soluble NFL that became insoluble in PBS in the $A\beta_{25-35}$ group was extensively nitrated (Fig. 7D), and the intensity of nitration was associated with the level of the PBS-insoluble, Triton X-100-soluble NFL (Fig. 7E). These results revealed new possibilities for Triton X-100-insolubile NFL in association with extensive nitration.

The Cell Numbers in the Hippocampus of Mice with the Impairment of Memory Induced by $A\beta_{25-35}$. On day 5 after the i.c.v. injection of $A\beta_{25-35}$, cell numbers in CA1, CA3, and the granular layer of the dentate gyrus of the hippocampal formation were examined using cresyl violet staining. The quantification of the stained cells revealed no cell loss induced by $A\beta_{25-35}$ (Table 2). These results were consistent with reports that at a dose of 3 to 5 μg, $A\beta_{25-35}$ could induce memory impairment but not cell loss within a time session of 1 month after its injection in mice (Maurice et al., 1996; Tohda et al., 2003). These results suggest that cell loss was not involved in the impairment of memory induced by $A\beta_{25-35}$ in mice.

Discussion

Neuronal oxidative damage has long been hypothesized as a critical mechanism of cellular dysfunction in neurodegenerative ailments (Perry et al., 2002). Reports showing that antioxidants delay or reduce progressive cognitive decline in both animal models and humans have emphasized the direct contribution of oxidative damage to cognitive pathology (Sano et al., 1997; Yamada et al., 1999; Lim et al., 2001). Oxidative damage is generally manifested by the increase of lipid peroxidation, DNA oxidation, protein oxidation, and peroxynitrite-mediated tyrosine nitration of proteins. The increased nitration of tyrosine could irreversibly disrupt the function of proteins (Koppal et al., 1999), and it might play a key pathogenic role in the progression of cognitive impairment (Smith et al., 1997; Keller, 2006). Until now, various proteins with tyrosine nitration have been reported in association with neurodegeneration and cognitive decline (Strong et al., 1998; Castegna et al., 2003; Tran et al., 2003; Sacksteder et al., 2006; Sultana et al., 2006). The diversity of nitrated proteins in these reports seems to depend on the species of the sources of samples (Sacksteder et al., 2006;

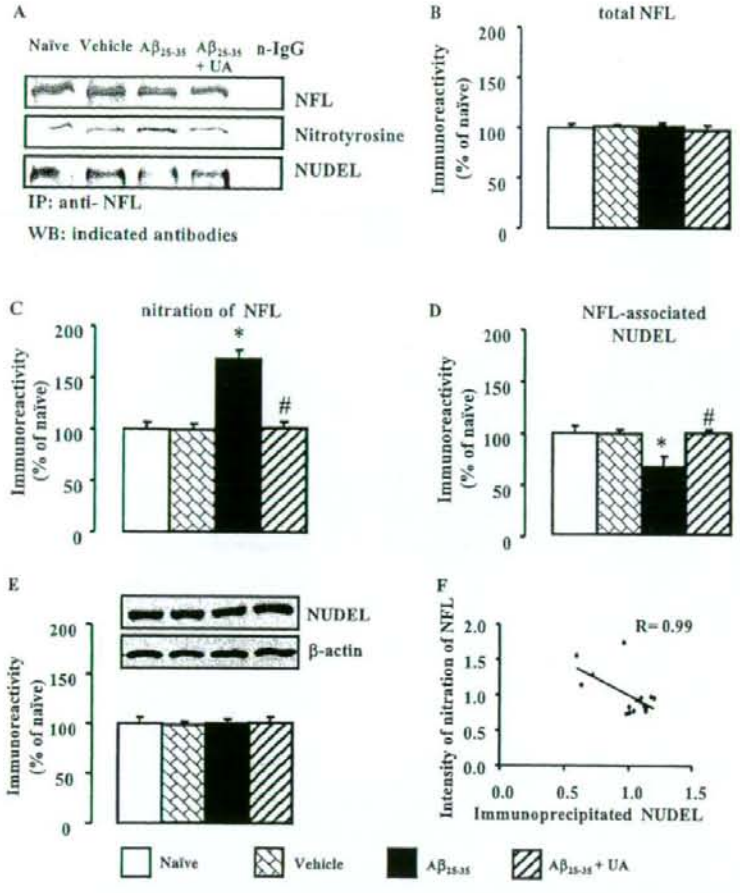

Fig. 5. Association between the extensive nitration of NFL and the reduced interaction with NUDEL in the Triton X-100-soluble fraction. A, the immunocomplexes obtained with the anti-NFL antibody, from precleared protein samples of the hippocampal homogenates, were separated by SDS-PAGE, blotted onto a PVDF membrane, and probed with the indicated antibodies. B, equal amounts of NFL protein were obtained. C, tyrosine nitration of NFL was increased in the $A\beta_{25-35}$ group, whereas UA treatment prevented the increase. D, the level of NFL-interacting NUDEL was reduced in the $A\beta_{25-35}$ group, whereas UA treatment prevented the reduction. E, no difference in NUDEL protein expression was found among the groups. F, the increased nitration of NFL was associated with reduced interaction with NUDEL. The intensity of bands was quantified and expressed as a percentage of that in the naive group. Data were presented as the mean ± S.E. ($n = 4$). *, $p < 0.05$ versus naive and vehicle; #, $p < 0.05$ versus $A\beta_{25-35}$.

Sultana et al., 2006), the proteomic detections on various conditions (Castegna et al., 2003; Sultana et al., 2006), immunodetections by means of different anti-nitrotyrosine antibodies with the diverse recognition property for nitrotyrosine (Strong et al., 1998; Tran et al., 2003), or the biological selectivity of tyrosine nitration (Ischiropoulos, 2003; Sacksteder et al., 2006). Dissimilar reports about the nitrated proteins in the brains of humans with Alzheimer's disease (AD) (Castegna et al., 2003; Sultana et al., 2006) emphasize the importance of the sources of protein, even in the same species or under the same conditions of detection during the identification process, while illustrating the diversity of nitration due to the dissimilar expression of proteins during the different stages of the disease.

In the present study, we looked for further evidence for the pathogenic role of protein nitration as one of the key contributors to the decline of cognitive function induced by Aβ. Using LC-MS/MS and immunodetection, we identified the hippocampal proteins with nitrated tyrosine residues after the i.c.v. injection of $A\beta_{25-35}$ in mice. Preferentially, in respect with currently examined proteins, intense nitration of NFL was observed, demonstrating a good correlation with the severity of cognitive impairment induced by $A\beta_{25-35}$.

NFL, one of the three subunits of NF proteins, is the indispensable core of the NF assembly (Zhu et al., 1997). Studies have reported that NFL is selectively nitrated compared with the majority of other proteins present in brain homogenates, and they suggested that newly synthesized free NFL is particularly susceptible to peroxynitrite-mediated nitration (Crow et al., 1997; Strong et al., 1998). The extensively nitrated NFL inhibits the assembly of unmodified NF subunits (Crow et al., 1997). On the other hand, the extensive serine phosphorylation of NFL could sufficiently block NF assembly (Nixon and Shea, 1992; Gibb et al., 1996). Therefore, we have evaluated the effect of tyrosine nitration on the phosphorylation of NFL at serine residues in general. The increased tyrosine nitration of NFL was associated with its serine hyperphosphorylation. Prevention of the extensive nitration of NFL by UA, a scavenger of $ONOO^-$ that nitrates proteins, restrained the serine phosphorylation of NFL at a normal level. The results indicated that the increased nitration of NFL could give rise to its serine hyperphosphorylation.

NFL requires direct binding with NUDEL, whereas NUDEL can not directly bind with other subunits of NF proteins, to initiate the assembly of NF (Nguyen et al., 2004). After the assembly of the NF network, NUDEL remains bound to the assembled Triton X-100-insoluble neurofilaments and may promote, in conjunction with molecular mo-

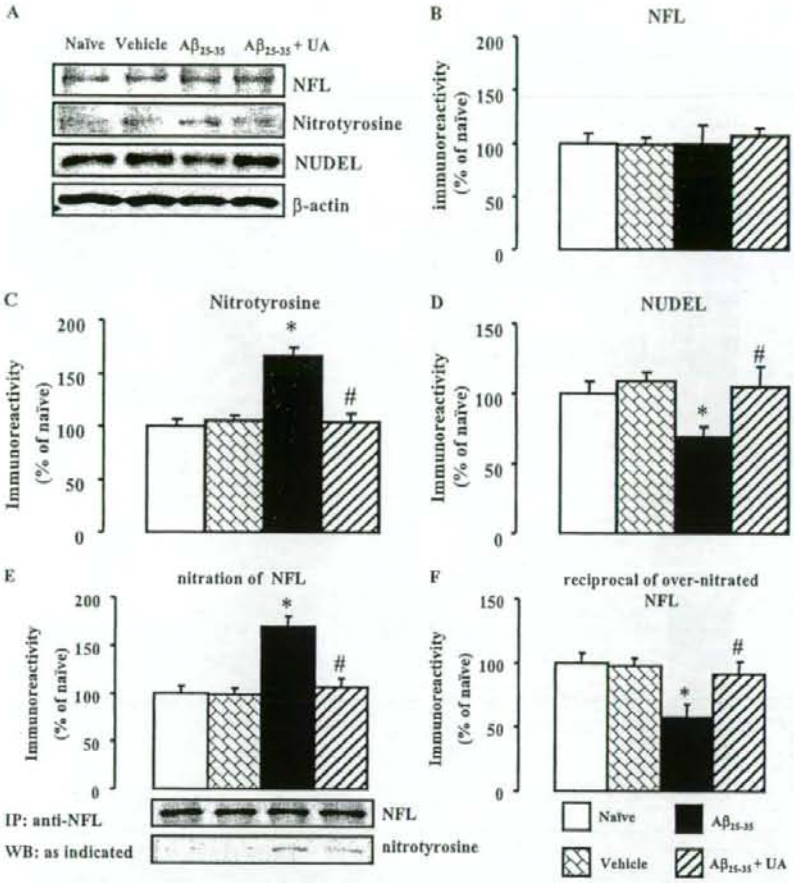

Fig. 6. The reduced content of NUDEL in the Triton X-100-insoluble cytoskeletal fraction. The Triton X-100-insoluble fraction, including cytoskeletal proteins, was solubilized in 6 M urea. A, equal amounts of protein were subjected to Western blot analysis. B, the protein levels of NFL were unchanged in all groups. C, the intensity of nitrotyrosine was increased in the $A\beta_{25-35}$ group, and the increase was prevented by UA, a scavenger of $ONOO^-$ that nitrates tyrosine. D, the protein level of NUDEL was reduced in the $A\beta_{25-35}$ group, and UA prevented this reduction. The quantified intensity of the bands was corrected by that of β-actin and expressed as a percentage of that in the naive group. E, equal amounts of NFL protein were immunoprecipitated and probed with anti-nitrotyrosine antibodies. The intensity of nitrotyrosine in NFL was increased in the $A\beta_{25-35}$ group, whereas UA prevented any increase. F, the reciprocal of the overnitrated NFL was estimated by applying multiplicative inverse (or reciprocal, in which the reciprocal of n is 1/n). The intensity of bands was quantified and expressed as a percentage of that in the naive group. Data are presented as the mean ± S.E. ($n = 4$). *, $p < 0.05$ versus naive and vehicle; #, $p < 0.05$ versus $A\beta_{25-35}$.

tors, the axonal transport of the neurofilaments (Nguyen et al., 2004). Thus, the level of interaction between NFL and NUDEL in the Triton X-100-soluble cytoplasmic fraction could be reflected by their protein levels in the Triton X-100-insoluble cytoskeletal fraction. In the current study, the increased nitration of Triton X-100-soluble NFL proteins in the $A\beta_{25-35}$ group was associated with its decreased interaction with NUDEL. In the Triton X-100-insoluble fraction, the protein level of NUDEL was reduced in the $A\beta_{25-35}$ group, and the reduction was prevented by treatment with UA. In the same fraction, the protein level of NFL surprisingly did not differ among groups, whereas the intensity of the nitration of NFL was strong in $A\beta_{25-35}$ group. Estimation by the multiplicative inverse approach indicated that the reduced level of nonextensively nitrated NFL in the $A\beta_{25-35}$ group parallels with that of NUDEL. These results required an explanation for the detection of the extensively nitrated NFL in the Triton X-100-insoluble cytoskeletal fraction, because the assembled NFL is nitration-resistant and the intensely nitrated NFL can not participate in the NF assembly (Crow et al., 1997). The alteration of the solubility of the overnitrated NFL might be involved in the detection of the extensively nitrated NFL in the Triton X-100-insoluble cytoskeletal fraction in the $A\beta_{25-35}$ group. Interpretation of the emergence of the intensely nitrated NFL in PBS-insoluble, but Triton X-100-soluble, protein pools in the $A\beta_{25-35}$ group indicates that extensive nitration would render NFL protein to have poor solubility in PBS. By this rate, it is possible that a considerable level of overnitrated NFL protein in the $A\beta_{25-35}$ group would even become Triton X-100 insoluble over a period of time, and that it would be detected along with a reduced level of NUDEL-associated assembled NFL, which is also Triton X-100 insoluble. The observation of detectable levels of nitration in NFL in the RIPA-soluble, Triton X-100-soluble, and Triton X-100-insoluble fractions in the naive and vehicle groups implies that natural nitration of tyrosine, as serine phosphorylation, might exist as a physiological property of NFL and might not be detrimental to the function of the protein, whereas extensive nitration is detrimental. The nitration-susceptible tyrosine residues of NFL are identified particularly as tyrosine 17 in the head region and tyrosines 138, 177, and 265 in the α-helical coil regions of the rod domain of the protein (Crow et al., 1997). It needs to be determined which tyrosine residue is the site for natural nitration or for extensive nitration. It has been reported that, although the exact mechanism is not clear, the newly synthesized Triton X-100-soluble NF proteins, including NFL, could separately undergo axonal transport before being in-

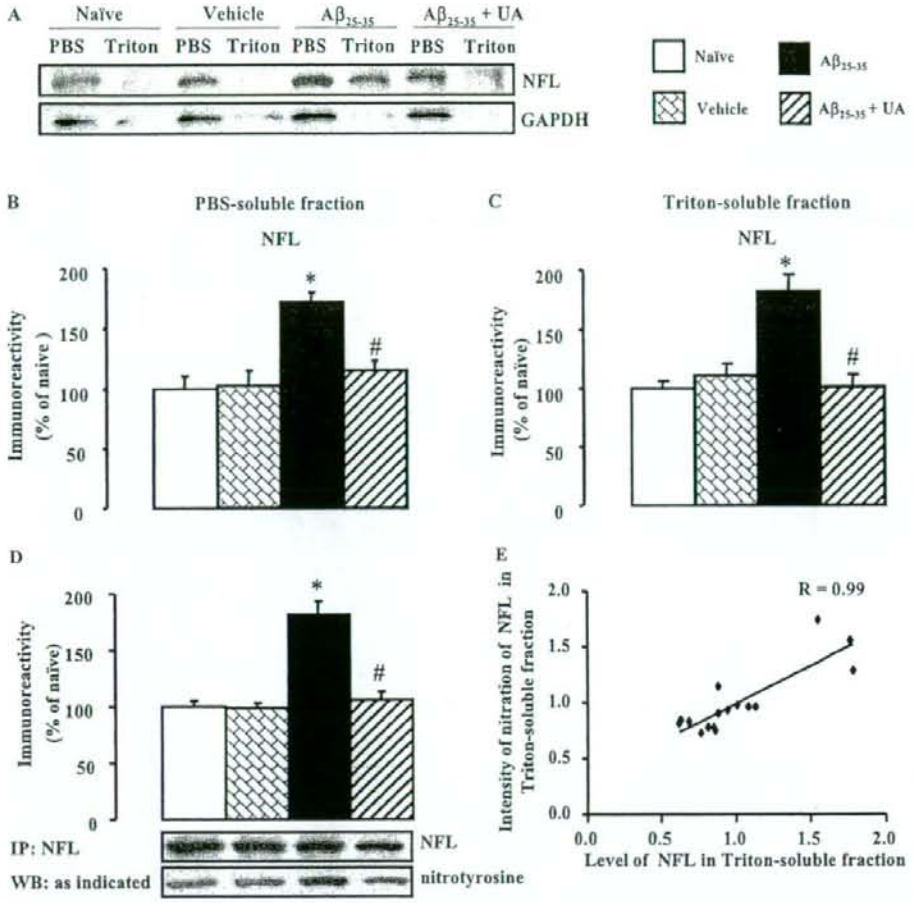

Fig. 7. The association of the extensive nitration of NFL with the alteration of solubility. The hippocampal tissues were homogenated in PBS and centrifuged at 13000*g* for 20 min, the washed pellets were solubilized in Triton X-100 as described under *Materials and Methods*, and equal amounts of protein were subjected to Western blot analysis. A to C, a majority of NFL and GAPDH proteins were soluble in PBS. NFL protein in the $A\beta_{25-35}$ group in both the PBS-soluble fraction and the Triton X-100-soluble fraction was increased, and the increase was prevented by UA, a scavenger of $ONOO^-$ that nitrates tyrosine. The quantified intensity of the bands was corrected by that of GAPDH and expressed as a percentage of that in the naive group. D, equal amounts of NFL from the Triton X-100-soluble proteins were immunoprecipitated and probed with anti-nitrotyrosine antibodies. The intensity of nitrotyrosine in NFL was increased in the $A\beta_{25-35}$ group, whereas UA prevented the increase. The intensity of bands was quantified and expressed as a percentage of that in the naive group. E, the level of NFL in the Triton X-100-soluble (PBS-insoluble) fraction was associated with the intensity of its nitration. Data are presented as the mean ± S.E. ($n = 4$). *, $p < 0.05$ versus naive and vehicle; #, $p < 0.05$ versus $A\beta_{25-35}$.

TABLE 2
The Nissl-positive cells in the hippocampus
In each group, $n = 4$.

Subfields of Hippocampus	Number of Nissl-Positive Cells			
	Naive	Vehicle	$A\beta_{25-35}$	$A\beta_{25-35}$ + UA
	counts/mm²			
CA1	10800 ± 230	10900 ± 290	10850 ± 250	10790 ± 270
CA3	6750 ± 190	6690 ± 210	6698 ± 180	6680 ± 310
GrDG	21000 ± 670	20980 ± 590	20990 ± 710	20780 ± 690

GrDG, the granular layer of the dentate gyrus.

corporated into the Triton X-100-insoluble axonal cytoskeleton (Jung et al., 1998). We do not know whether the NFL proteins with natural nitration undergo axonal transport after the NF assembly or undergo axonal transport before being incorporated into the Triton X-100-insoluble axonal cytoskeleton.

The observation of no cell loss in CA1, CA3, and the granular layer of the dentate gyrus of the hippocampus in mice

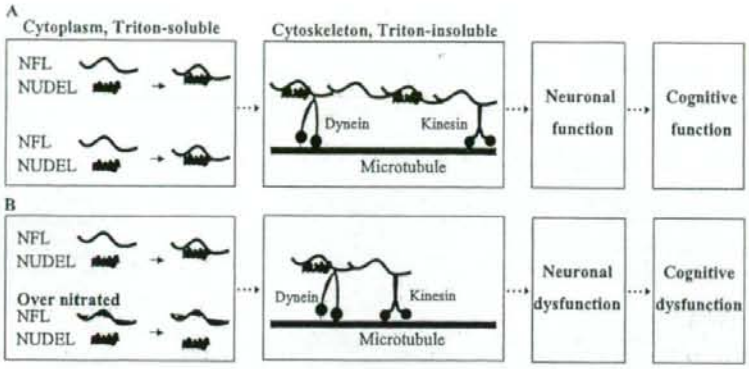

Fig. 8. The contribution of the extensive nitration of NFL to cognitive dysfunction. A, in this model, NFL interacts with NUDEL, which is essential for the incorporation of NF subunits into the network during NF assembly and elongation. A normal NF assembly and elongation favors normal neuronal and cognitive functions. B, the overnitration of NFL disrupts the interaction of NFL with NUDEL and may lead to the defective assembly of NF and abnormalities in neuronal and cognitive functions. The resized microtubules, kinesin, and dyenin have been added for clarity (modified from Nguyen et al., 2004; Holzbaur, 2004).

that received $A\beta_{25-35}$ injections favored the contribution of extensive nitration of NFL to the impairment of memory. A recent study demonstrated that rapidly formed fresh amyloid plaques cause axonal and dendritic structural changes within a minimum of 5 days after the "birth of the plaques" (Meyer-Luehmann et al., 2008). Given the time windows of Aβ neurotoxicity, $A\beta_{25-35}$ may require longer time to cause cell loss in our mouse model of cognitive impairment.

The disrupted interaction between NFL and NUDEL is regarded as the most important factor for the destabilization of the NF assembly that leads to the axonal dysfunction, which is an early event in the cognitive pathology of AD (Nguyen et al., 2004; Stokin et al., 2005). Therefore, our results suggest that disrupted interaction between NUDEL and NFL with extensive nitration could be one of the major factors that associated with the cognitive dysfunction induced by Aβ in mice (Fig. 8). However, further studies are required to investigate whether the extensive nitration of NFL and the impaired interaction with NUDEL induced by Aβ are associated with the disruption of axonal transport.

Acknowledgments

We are grateful to Dr. Minh Dang Nguyen for discussions on the sample preparation.

References

Alkam T, Nitta A, Mizoguchi H, Itoh A, and Nabeshima T (2007) A natural scavenger of peroxynitrites, rosmarinic acid, protects against impairment of memory induced by Aβ25–35. *Behav Brain Res* **180**:139–145.

Alkam T, Nitta A, Mizoguchi H, Saito K, Seshima M, Itoh A, Yamada K, and Nabeshima T (2008) Restraining tumor necrosis factor-alpha by thalidomide prevents the amyloid beta-induced impairment of recognition memory in mice. *Behav Brain Res* **189**:100–106.

Andersen JK (2004) Oxidative stress in neurodegeneration: cause or consequence? *Nat Med* **10**:S18–S25.

Aoyama Y and Kitajima Y (1999) Pemphigus vulgaris-IgG causes a rapid depletion of desmoglein 3 (Dsg3) from the Triton X-100 soluble pools, leading to the formation of Dsg3-depleted desmosomes in a human squamous carcinoma cell line, DJM-1 cells. *J Invest Dermatol* **112**:67–71.

Bastianetto S and Quirion R (2004) Natural antioxidants and neurodegenerative diseases. *Front Biosci* **9**:3447–3452.

Black MM, Keyser P, and Sobel E (1986) Interval between the synthesis and assembly of cytoskeletal proteins in cultured neurons. *J Neurosci* **6**:1004–1012.

Castegna A, Thongboonkerd V, Klein JB, Lynn B, Markesbery WR, and Butterfield DA (2003) Proteomic identification of nitrated proteins in Alzheimer's disease brain. *J Neurochem* **85**:1394–1401.

Crow JP, Ye YZ, Strong M, Kirk M, Barnes S, and Beckman JS (1997) Superoxide dismutase catalyzes nitration of tyrosines by peroxynitrite in the rod and head domains of neurofilament-L. *J Neurochem* **69**:1945–1953.

Dalle-Donne A, Scaloni D, Giustarini E, Cavarra G, Tell G, Lungarella R, Colombo R, Rossi R, and Milzani A (2005) Proteins as biomarkers of oxidative/nitrosative stress in diseases: the contribution of redox proteomics. *Mass Spectrom Rev* **24**: 55–99.

Gibb BJ, Robertson J, and Miller CC (1996) Assembly properties of neurofilament light chain Ser55 mutants in transfected mammalian cells. *J Neurochem* **66**:1306–1311.

Hisanaga S, Gonda Y, Inagaki M, Ikai A, and Hirokawa N (1990) Effects of phosphorylation of the neurofilament L protein on filamentous structures. *Cell Regul* **1**:237–248.

Holzbaur EL (2004) Tangled NUDELs? *Nat Cell Biol* **6**:569–570.

Ischiropoulos H (2003) Biological selectivity and functional aspects of protein tyrosine nitration. *Biochem Biophys Res Commun* **305**:776–783.

Jung C, Yabe J, Wang FS, and Shea TB (1998) Neurofilament subunits can undergo axonal transport without incorporation into Triton-insoluble structures. *Cell Motil Cytoskeleton* **40**:44–58.

Keller JN (2006) Oxidative damage and oxidative stress in Alzheimer's disease. *Res Pract Alzheimer's Dis* **11**:110–114.

Kim HC, Yamada K, Nitta A, Olariu A, Tran MH, Mizuno M, Nakajima A, Nagai T, Kamei H, Jhoo WK, et al. (2003) Immunocytochemical evidence that amyloid beta (1–42) impairs endogenous antioxidant systems in vivo. *Neuroscience* **119**:399–419.

Koppal T, Drake J, Yatin S, Jordan B, Varadarajan S, Bettenhausen L, and Butterfield DA (1999) Peroxynitrite-induced alterations in synaptosomal membrane proteins: insight into oxidative stress in Alzheimer's disease. *J Neurochem* **72**:310–317.

Kubo T, Nishimura S, Kumagae Y, and Kaneko I (2002) In vivo conversion of racemized beta-amyloid ([D-Ser 26]A beta 1–40) to truncated and toxic fragments ([D-Ser 26]A beta 25–35/40) and fragment presence in the brains of Alzheimer's patients. *J Neurosci Res* **70**:474–483.

Lim GP, Chu T, Yang F, Beech W, Frautschy SA, and Cole GM (2001) The curry spice curcumin reduces oxidative damage and amyloid pathology in an Alzheimer transgenic mouse. *J Neurosci* **21**:8370–8377.

Maurice T, Lockhart BP, and Privat A (1996) Amnesia induced in mice by centrally administered beta-amyloid peptides involves cholinergic dysfunction. *Brain Res* **706**:181–193.

Meyer-Luehmann M, Spires-Jones TL, Prada C, Garcia-Alloza M, de Calignon A, Rozkalne A, Koenigsknecht-Talboo J, Holtzman DM, Bacskai BJ, and Hyman BT (2008) Rapid appearance and local toxicity of amyloid-beta plaques in a mouse model of Alzheimer's disease. *Nature* **451**:720–724.

Nabeshima T, Katoh A, Ishimaru H, Yoneda Y, Ogita K, Murase K, Ohtsuka H, Inari K, Fukuta T, and Kameyama T (1991) Carbon monoxide-induced delayed amnesia, delayed neuronal death and change in acetylcholine concentration in mice. *J Pharmacol Exp Ther* **256**:378–384.

Nguyen MD, Shu T, Sanada K, Larivière RC, Tseng HC, Park SK, Julien JP, and Tsai LH (2004) A NUDEL-dependent mechanism of neurofilament assembly regulates the integrity of CNS neurons. *Nat Cell Biol* **6**:595–608.

Nitta A, Fukuta T, Hasegawa T, and Nabeshima T (1997) Continuous infusion of beta-amyloid protein into the rat cerebral ventricle induces learning impairment and neuronal and morphological degeneration. *Jpn J Pharmacol* **73**:51–57.

Nixon RA and Shea TB (1992) Dynamics of neuronal intermediate filaments: a developmental perspective. *Cell Motil Cytoskeleton* **22**:81–91.

Perry G, Nunomura A, Hirai K, Zhu X, Pérez M, Avila J, Castellani RJ, Atwood CS, Aliev G, Sayre LM, et al. (2002) Is oxidative damage the fundamental pathogenic mechanism of Alzheimer's and other neurodegenerative diseases? *Free Rad Biol Med* **33**:1475–1479.

Pike CJ, Walencewicz-Wasserman AJ, Kosmoski J, Cribbs DH, Glabe CG, and Cotman CW (1995) Structure-activity analyses of Aβ peptides: contributions of the β25–35 region to aggregation and neurotoxicity. *J Neurochem* **64**:253–265.

Reynolds MR, Berry RW, and Binder LI (2007) Nitration in neurodegeneration: deciphering the "Hows" "nYs". *Biochemistry* **46**:7325–7336.

Sacksteder CA, Qian WJ, Knyushko TV, Wang H, Chin MH, Lacan G, Melega WP, Camp DG 2nd, Smith RD, Smith DJ, et al. (2006) Endogenously nitrated proteins in mouse brain: links to neurodegenerative disease. *Biochemistry* **45**:8009–8022.

Sano M, Ernesto C, Thomas RG, Klauber MR, Schafer K, Grundman M, Woodbury P, Growdon J, Cotman CW, Pfeiffer E, et al. (1997) A controlled trial of selegiline, alpha-tocopherol, or both as treatment for Alzheimer's disease. The Alzheimer's Disease Cooperative Study. *N Engl J Med* **336**:1216–1222.

Silberberg JS (1990) Estimating the benefits of cholesterol lowering: are risk factors for coronary heart disease multiplicative? *J Clin Epidemiol* **43**:875–879.

Smith MA, Richey Harris PL, Sayre LM, Beckman JS, and Perry G (1997) Wide-

spread peroxynitrite-mediated damage in Alzheimer's disease. *J Neurosci* **17**: 2653–2657.
Stokin GB, Lillo C, Falzone TL, Brusch RG, Rockenstein E, Mount SL, Raman R, Davies P, Masliah E, Williams DS, et al. (2005) Axonopathy and transport deficits early in the pathogenesis of Alzheimer's diseases. *Science* **307**:1282–1288.
Strong MJ, Sopper MM, Crow JP, Strong WL, and Beckman JS (1998) Nitration of the low molecular weight neurofilament is equivalent in sporadic amyotrophic lateral sclerosis and control cervical spinal cord. *Biochem Biophys Res Commun* **248**:157–164.
Sultana R, Poon HF, Cai J, Pierce WM, Merchant M, Klein JB, Markesbery WR, and Butterfield DA (2006) Identification of nitrated proteins in Alzheimer's disease brain using a redox proteomics approach. *Neurobiol Dis* **22**:76–87.
Tohda C, Tamura T, and Komatsu K (2003) Repair of amyloid beta (25–35)-induced memory impairment and synaptic loss by a Kampo formula, Zokumei-to. *Brain Res* **990**:141–147.
Tran MH, Yamada K, Nakajima A, Mizuno M, He J, Kamei H, and Nabeshima T (2003) Tyrosine nitration of a synaptic protein synaptophysin contributes to amyloid β-peptide-induced cholinergic dysfunction. *Mol Psychiatry* **8**:407–412.
Walsh DM and Selkoe DJ (2004) Deciphering the molecular basis of memory failure in Alzheimer's disease. *Neuron* **44**:181–193.
Yamada K, Tanaka T, Han D, Senzaki K, Kameyama T, and Nabeshima T (1999) Protective effects of idebenone and alpha-tocopherol on beta-amyloid-(1–42)-induced learning and memory deficits in rats: implication of oxidative stress in beta-amyloid-induced neurotoxicity in vivo. *Eur J Neurosci* **11**:83–90.
Zhu Q, Couillard-Després S, and Julien JP (1997) Delayed maturation of regenerating myelinated axons in mice lacking neurofilaments. *Exp Neurol* **148**:299–316.

Address correspondence to: Dr. Toshitaka Nabeshima, Department of Chemical Pharmacology, Graduate School of Pharmaceutical Science, Meijo University, Nagoya 468-8503, Japan. E-mail: tnabeshi@ccmfs.meijo-u.ac.jp

JPET PHARMACOLOGY AND EXPERIMENTAL THERAPEUTICS aspet

Molecular Psychiatry (2008) 13, 451–463

www.nature.com/mp

ORIGINAL ARTICLE

Identification of Piccolo as a regulator of behavioral plasticity and dopamine transporter internalization

X Cen[1,2], A Nitta[1], D Ibi[1,3], Y Zhao[1], M Niwa[1], K Taguchi[1], M Hamada[1], Y Ito[3], Y Ito[4], L Wang,[2] and T Nabeshima[1,5]

[1]Department of Neuropsychopharmacology and Hospital Pharmacy, Nagoya University Graduate School of Medicine, Nagoya, Japan; [2]National Chengdu Center for Safety Evaluation of Drugs, West China Hospital, Sichuan University, Chengdu, China; [3]Department of Pharmacology, College of Pharmacy, Nihon University, Chiba, Japan; [4]Equipment Center for Research and Education, Nagoya University Graduate School of Medicine, Nagoya, Japan and [5]Department of Chemical Pharmacology, Meijo University Graduate School of Pharmaceutical Sciences, Nagoya, Japan

Dopamine transporter (DAT) internalization is a mechanism underlying the decreased dopamine reuptake caused by addictive drugs like methamphetamine (METH). We found that Piccolo, a presynaptic scaffolding protein, was overexpressed in the nucleus accumbens (NAc) of the mice repeatedly administrated with METH. Piccolo downexpression by antisense technique augmented METH-induced behavioral sensitization, conditioned reward and synaptic dopamine accumulation in NAc. Expression of Piccolo C_2A domain attenuated METH-induced inhibition of dopamine uptake in PC12 cells expressing human DAT. Consistent with this, it slowed down the accelerated DAT internalization induced by METH, thus maintaining the presentation of plasmalemmal DAT. In immunostaining and structural modeling Piccolo C_2A domain displays an unusual feature of sequestering membrane phosphatidylinositol 4,5-bisphosphate, which may underlie its role in modulating DAT internalization. Together, our results indicate that Piccolo upregulation induced by METH represents a homeostatic response in the NAc to excessive dopaminergic transmission. Piccolo C_2A domain may act as a cytoskeletal regulator for plasmalemmal DAT internalization, which may underlie its contributions in behavioral plasticity.
Molecular Psychiatry (2008) **13,** 451–463; doi:10.1038/sj.mp.4002132; published online 15 January 2008

Keywords: Piccolo; dopamine transporter; methamphetamine; behavioral plasticity; C_2A domain

Introduction

Dopamine transporter (DAT), a member of the Na^+/Cl^--dependent transporters in the dopaminergic neurons, is critical for terminating dopamine (DA) neurotransmission and contributes to the abuse potential of psychostimulants. The stimulating and reinforcing effects of drugs result from enhanced synaptic DA accumulation in specific brain areas like nucleus accumbens (NAc). Cocaine and methamphetamine (METH; or its analogue amphetamine) elevate extracellular DA by inhibiting DA reuptake through DAT and, in the case of METH, also by promoting reverse transport of nonvesicular DA, reducing plasma membrane DAT through internalization, and displacing DA from synaptic vesicle (SV) to the cytoplasm.[1,2]

Membrane trafficking of DAT is closely associated with DA homeostasis and synaptic plasticity, and increasing evidences have showed that METH-like drugs are able to modulate this dynamic process.[3] The internalization of plasmalemmal DAT is a clathrin-mediated process,[4,5] and internalized DAT can be sorted to endosomal compartments where they may be recycled to cell surface and/or lysosome for degradation.[6] Inhibition of endocytic machinery assembly can attenuate amphetamine- or phorbol ester-mediated DAT internalization,[7] whereas expression of endosomal proteins like Rab5 in endosomal vesicles promotes amphetamine-induced intracellular DAT accumulation.[8] These findings strongly suggest that manipulation of endocytic components could be an important manner for regulating DAT internalization.

Piccolo, a component of the presynaptic cytoskeletal matrix, is assembled ultrastructurally as an electron-dense region of filaments at the active zone (AZ). It is proposed to play a scaffolding role in regulating AZ assembly,[9] actin cytoskeleton and SV trafficking.[10,11] Piccolo contains multiple subdomains including PDZ domain and Ca^{2+}/phospholipid binding (C_2A and C_2B) domains, each of which exhibits

Correspondence: Professor T Nabeshima, Department of Chemical Pharmacology, Meijo University Graduate School of Pharmaceutical Sciences, 150 Yagotoyama, Tenpaku, Nagoya 468-8503, Japan.
E-mail: tnabeshi@ccmfs.meijo-u.ac.jp
Received 17 June 2007; revised 14 September 2007; accepted 21 September 2007; published online 15 January 2008

distinctive features.[10,12] PDZ domain may interact with other presynaptic molecules involving molecule anchoring and assembly at AZ.[13] C_2A domain shows an unusual ability to sense intracellular changes of Ca^{2+} levels and then trigger the association with membrane phospholipids (PIs) via electrostatic interaction.[14] Notably, it interacts with phosphatidylinositol 4,5-bisphosphate (PIP_2),[15] a critical molecule for actin dynamics and endocytosis. It is well established that PIP_2 coordinates membrane fusion with actin filament to promote membrane movement, and recruits accessory adaptors for clathrin-coated pits.[16] Therefore, modulation of plasmalemmal PIP_2 may affect PIP_2-dependent biological processes like membrane trafficking and endocytosis.

In this study we find that Piccolo servers as a negative presynaptic modulator for behavioral hypersensitivity and blunts excessive dopaminergic synaptic plasticity by regulating plasmalemmal DAT internalization. Moreover, Piccolo C_2A domain may contribute to such distinct effects by targeting membrane PIP_2.

Materials and methods

Material

A pCMV-hDAT expression plasmid was kindly provided by Dr Marc Caron (Duke University Medical Center). The expression plasmids of pCMV-HA-Piccolo-PDZ (amino acid 3900–4244), pCMV-Myc-Piccolo-C_2A (amino acid 4704–5610) and pGEX4T-GST-p13192 (amino acid 4364–4755; named p13192) were constructed as previously described.[17] The following antibodies were used: hDAT and tyrosine hydroxylase (TH; Chemicon International Inc., Billerica, MA); hemagglutinin epitope (HA) and c-Myc (Cell Signaling, Billerica, MA); GST (Amersham Biosciences, Uppsala, Sweden); Piccolo and Rim 2 (Synaptic Systems, Albany, OR); PIP_2 (Assay Designs, Ann Arbor, MI, USA); syntaxin 1A (Santa Cruz Biotechnology, Santa Cruz, CA); synaptophysin (Sigma-Aldrich, St Louis, MO). The following reagents were used: botulinum neurotoxin (Bont)/C1 and Bont/B (Wako Pure Chemical Industries Ltd, Osaka, Japan); sulfo-NHS-biotin and immobilized streptavidin (Pierce, Rockford, IL).

RT–PCR and real-time RT–PCR

Isolation of total RNA from the NAc of mice was performed using RNeasy Mini Kit (QIAGEN, Hilden, Germany). The mRNA productions from nine target cDNA sequences of Piccolo were assayed by reverse transcription (RT)–PCR, followed by electrophoresis. The forward and reverse primers for the nine sequences were shown in Supplementary Table 1. Piccolo mRNA levels in brain NAc were validated by quantitative real-time RT–PCR using an iCycler System (Bio-Rad, Hercules, CA). Briefly, isolation of total RNA was performed using RNeasy Mini Kit (QIAGEN). For reverse transcription, 1 μg RNA was converted into a cDNA by a standard 20 μl reverse transcriptase reaction using oligo (dT) primers (Invitrogen, Hercules, CA) and Superscript II RT (Bio-Rad Laboratories, Hercules, CA, USA). Total cDNA (1 μl) was amplified in a 25 μl reaction mixture using 0.1 μM each of forward and reverse primers and Platinum Quantitative PCR SuperMix-UDG (Invitrogen). The primer and dye probes were designed by Nippon Gene Co. Ltd (Tokyo, Japan) using Primer Express software. The forward primer was 5′-GGATAGCGCACAAGGTTTTCC-3′ (base pair 4180–4200) with reverse being 5′-TTCAACCGAAT CATAGGATGCTC-3′ (base pair 4257–4279), and the dye probe was 5′-CACAAAGAGAATCCTGAGCTGG TCGATGA-3′ (base pair 4192–4220). Ribosomal mRNA was used and determined as control for RNA integrity with TaqMan ribosomal RNA control reagents.

Antisense

An antisense oligodeoxynucleotide (AS; 5′-CTCTGCC AAAACTTC-3′) and a scramble oligodeoxynucleotide (SC; 5′-AACGTAGTCACGTAG-3′) were synthesized by Nippon Gene Co. Ltd. C57BL/6 mice were infused intracerebroventricularly with AS or SC (1 μl h^{-1}, 10 nmol ml^{-1}), made in regular artificial cerebrospinal fluid (CSF) or CSF alone, using an implanted Alzet minipump (AP −0.5 mm, ML +1.0 mm from bregma, DV −2.0 mm from the skull).

Locomotor activity and CPP Test

Locomotor activity was measured using an infrared detector (Neuroscience, Tokyo, Japan) as our previous report.[18] The mice were injected with METH (1 mg kg^{-1}, s.c.) daily for 5 days (day 1–5), followed by locomotor activity measurement at days 1, 3 and 5. Conditioned place-preference (CPP) test was carried out according to the methods as described before but with modification in conditioning.[19] Briefly, a mouse was allowed to move freely between transparent and black boxes for 20 min once per day for 3 days (from day 2 to day 0) in the preconditioning. In the mornings from days 1 to 3, the mouse was treated with METH (1 mg kg^{-1}, s.c.) and put in nonpreferred box for 20 min. After an interval of 12 h the mouse was treated with saline and put in the side opposite to the METH-conditioning box for 20 min. On day 4, the post-conditioning test was performed without drug treatment, and place-conditioning behavior was expressed as post-value minus pre-value.

Microdialysis

C57BL/6 mice were anesthetized before a guide cannula was implanted in the NAc (AP +1.7 mm, ML −0.8 mm from bregma, DV −4.0 mm from the skull).[19] Meanwhile, a mini osmotic pump filled with AS, SC (10 nmol ml^{-1}) or CSF was implanted intracerebroventricularly as described above. Equal numbers of animals were assigned to METH and saline pretreatment groups. Dialysis probes were inserted to the guide cannula the night prior to the experiment. Microdialysis samples were collected every 10 min (2.0 μl min^{-1}). The DA output was presented as